AN ABSTRACT OF THE THESIS OF

Jill E. Schrlau for the degree of Master of Science in Environmental Engineering presented on September 20, 2016.

Title: Transformation of Phenanthrene by *Mycobacterium* sp. ELW1 and the Formation of Toxic Metabolites.

Abstract approved:

_____

Lewis Semprini Staci Simonich

The ability of *Mycobacterium* sp. ELW1, a novel microbe capable of alkene oxidation, to co-metabolize phenanthrene (PHE) was studied. ELW1 was able to completely co-metabolize PHE, at different concentrations below its water solubility limit, in an aqueous environment. The alkene monooxygenases in ELW1, used to initiate oxidation of PHE, were effectively inhibited by 1-octyne despite some PHE transformation observed. PHE metabolites consisted of only hydroxyphenanthrenes (OHPHEs) with *trans*-9,10-dihydroxy-9,10-dihydrophenanthrene (*trans*-9,10-PHE), the primary product, comprising more than 90% of the total metabolites formed in both PHE-exposed cells and 1-octyne controls. Mass balance was estimated by summing the zero-order formation rates of OHPHE metabolites and comparing these to the zero-order transformation rates PHE in PHE-exposed cells. The transformation rates of PHE and were in good agreement with the formation rates of the metabolites. PHE transformation followed first-order rates that, when normalized by biomass, were in the range of those estimated by the ratio of the Michaelis-Menten kinetic

variables of maximum transformation rate (k_{max}) to the half-saturation constant (K_S). Estimated values for k_{max} to K_S obtained through both non-linear and linearization methods resulted in k_{max}/K_S estimates that were a factor of ~3 lower compared to experimental values. Both experimental and estimated values of k_{max}, K_S, and k_{max}/K_S were 2-3 magnitudes lower than literature values determined for microbes other than Mycobacterium sp. using different models that incorporated additional parameters. OHPHE standards, including 1-hydroxyphenanthrene (1-PHE), 3-hydroxyphenanthrene (3-PHE), 4-hydroxyphenanthrene (4-OHE), 9-hydroxyphenanthrene (9-PHE), and 1,9-dihydroxyphenanthrene (1,9-PHE), were developmentally toxic to embryonic zebrafish. However, PHE and *trans*-9,10- PHE. were not toxic. OHPHE metabolite mixtures formed by ELW1 were also tested for toxicity using embryonic zebrafish. The embryonic zebrafish were exposed to OHPHE metabolite mixtures that were at least 1.5 times less than the concentration need to elicit a toxic response. However, toxicity was observed in the two latest time points, 76 and 122 hr, in PHE-exposed cells. The toxicity may have been caused by an unidentified toxic metabolite.

Transformation of Phenanthrene by Mycobacterium sp. ELW1 and the Formation of Toxic Metabolites

by
Jill E. Schrlau

A THESIS

submitted to

Oregon State University

in partial fulfillment of
the requirements for the
degree of

Master of Science

Presented September 20, 2016
Commencement June 2017

Master of Science thesis of Jill E. Schrlau presented on September 20, 2016

APPROVED:

Major Professor, representing Environmental Engineering

Head of the School of Chemical, Biological, and Environmental Engineering

Dean of the Graduate School

I understand that my thesis will become part of the permanent collection of Oregon State University libraries. My signature below authorizes release of my thesis to any reader upon request.

Jill E. Schrlau, Author

ACKNOWLEDGEMENTS

The author expresses sincere appreciation to my support network consisting of CBEE graduate students who started this journey with me, and their significant others, (Hannah, Paige, Mark, Kristin, Lauren, Matt, Andy, and Ariel), the Semprini Lab group (Hannah, Emma, Marina, Paige, Kyle, Tanner, and Mohammad), and the Simonich Lab group, past and present (Amber, Justin, Cleo, Ivan, Lisandra, Anna, Leah, O, Carlos, Christopher, Scott, On, Carlos, Shelby, Julie, Sarah, and Glenn). The Simonich Lab has been my work family for 12 years now and even though the faces and personalities change, the support and positive attitudes always remain. A big thank you goes to my family for always supporting me in my life decisions even though they wished I made different ones.

Thank you to Lew Semprini for being willing to form a collaboration to make this work possible. I am extremely grateful to have been mentored by him.

Above all, my deepest appreciation and gratitude goes to my mentor in science (and sometimes life) and my friend for many years, Staci Simonich. With her encouragement and financial support, I was able to overcome several roadblocks and complete this journey for the second time.

Finally, I want to acknowledge the memories of those who are no longer with me but remain ever present in my heart and mind. Michael Elder, my Oregon Dad and best friend, and Chiyah, my sweet puppy whose companionship warmed my soul on the coldest days. My love for both of you is endless and I know we'll meet again in this life or the next.

CONTRIBUTION OF AUTHORS

Dr. Staci L. Massey Simonich and Dr. Lewis Semprini provided support and editorial comments for all sections of this thesis.

Chapter 2: Prepared by Jill E. Schrlau with editorial comments from Staci L. Massey Simonich and Lewis Semprini. Significant assistance with experiments and sample processing was provided by Amber Kramer. Zebrafish tested and advice was provided by Anna Chlebowski.

TABLE OF CONTENTS

TABLE OF CONTENTS (Continued)

LIST OF FIGURES

LIST OF TABLES

CHAPTER 1: INTRODUCTION

1.1 Polycyclic Aromatic Hydrocarbons (PAHs)

Polycyclic aromatic hydrocarbons (PAHs) are compounds comprised of two or more fused benzene rings that form during the incomplete combustion of organic substances from both natural and anthropogenic sources.[1] PAHs are found in asphalt,[2] crude oil,[3] coal tar,[4-6] and creosote.[7,8] Unsubstituted PAHs, commonly referred to as parent PAHs, vary in levels of toxicity, genotoxicity, mutagenicity and/or carcinogenic properties.[9] Low molecular weight (LMW) PAHs are those comprised of 2-3 rings and tend to be acutely toxic.[10] While high molecular weight (HMW) PAHs, structure with 4 or more rings, are both carcinogenic and genotoxic.[10,11] Many PAHs are considered to be probable or possible human and animal carcinogens by the International Agency for Research on Cancer (IARC) and also probable human carcinogens by the U.S. EPA Integrated Risk Information System.[9,12] Due to their ubiquity and known toxicity, The U.S. Environmental Protection Agency (EPA) includes 16 PAHs on their Priority Pollutant List.[13]

Once released into the environment, PAHs partition to different environmental compartments based on the compounds' physical chemical properties, including vapor pressure, water solubility, and the preferential accumulation between any two environmental compartments described by partition coefficients. The octanol-air partition coefficient, K_{OA}, describes the accumulation potential of PAHs to terrestrial surfaces, such as soil or vegetation, compared to the atmosphere. The octanol-water partition coefficient, K_{OW}, describes the affinity of PAHs to sediment or aquatic life

compared to water. Finally, the partitioning of PAHs between the aqueous phase and the atmosphere is described by Henry's Law Constant. As the number of rings for unsubstituted PAHs increase, vapor pressure and water solubility of PAHs decrease and their affinity to organic and lipophilic surfaces increase (Appendix A.1). Based on discharge data and physical chemical properties, PAH accumulation preferentially occurs in soil compared to other environmental compartments, including the atmosphere, inland water, sediments (fresh water only), vegetation, waste residue, and land biota.[14]

1.2 Remediation Technologies for PAHs

Many remediation technologies focus on removal of PAHs in soil due to their elevated accumulation in this compartment.[14] A thorough review of PAH remediation technologies has been published by Gan *et al.* (2009).[15] Briefly, these technologies include solvent extraction, thermal technologies, chemical oxidation, and bioremediation. Solvent extraction uses a fluid, such as solvents, mixture of solvents, surfactants, biodegradable agents, supercritical fluid, and subcritical fluid, to desorb PAHs from soil particles into the extraction fluid which is then separated from the soil. In thermal treatment, heat (870 to 1200^{o}C) is used to destroy or volatilize PAHs in soil. This technique often requires additional pollution control devices to control greenhouse gases produced during the process.[15] Chemical oxidation uses oxidation reactions to degrade PAHs. Common chemical oxidants used include Fenton's reagent, ozone, peroxy-acid, potassium permanganate, hydrogen peroxide, and activated sodium persulphate.[15] Bioremediation is the natural degradation of contaminants using organisms either in the presence of oxygen (aerobic) or without

oxygen (anaerobic). This thesis focuses on the use of aerobic microbial bioremediation of a single PAH, phenanthrene.

1.3 Aerobic Microbial Bioremediation

Several bioremediation strategies use aerobic microbes in either pure or mixed populations. These strategies include utilizing naturally-occurring microbial populations, biostimulation, and bioaugmentation *in situ* and/or *ex situ*. Biostimulation is the stimulation of naturally-occurring microbial communities through the modification of the environment by the addition of limiting agents like nutrients (N, P, C, and O) and pH using fertilizers, various types of composts, and tilling.[15-21] When endogenous bacteria are unable to degrade PAHs, the contaminated soil may undergo bioaugmentation through the addition of specific exogenous bacteria *in situ* and/or *ex situ*.[22,23] Once a contaminated site, or bioreactor, has been bioaugmented, biostimulation strategies may also be employed.

Several studies, utilizing these aerobic bioremediation strategies, have been conducted on the bioremediation of parent PAHs. Plant-based compost and slow release fertilizers were used as a biostimulant in PAH contaminated soil which resulted in increased removal rates of PAHs and improved meiofauna diversity.[16-18,21] Biostimulated soil from an oil well contaminated with total petroleum hydrocarbons (TPHs) showed a 60% removal after 10 weeks.[24] Bioaugmentation was performed in a comparative study by Festa *et al*. where soil was spiked with phenanthrene, a 3-ringed parent PAH, and was bioaugmented with a bacterial consortium, as well as with an isolated *Sphingobuim* sp. strain.[23] Although both bioaugmented scenarios resulted in complete removal of phenanthrene after 63 days, *Sphingobuim* sp. was

able to degrade 75% of phenanthrene in 7 days compared to the consortium which removed 58% [22]. The combination of both biostimulation and bioaugmentation on PAH removal has also been studied.[17] Mesocosm studies of bioaugmented and biostimulated sediments showed possible competition between endogenous and exogenous microbial populations, however this did not result in a difference in the removal rate of phenanthrene compared to biostimulated only sediments.[17] Singularly, or in combination, biostimulation and bioaugmention are promising bioremediation techniques for PAHs.

1.4 Transformation, Biodegradation, and Co-metabolism

Terms for different biodegradation processes are often used interchangeably in scientific literature. For the purpose of this thesis, transformation will refer to the general degradation of contaminants by microbial populations. Biodegradation will refer to the ability of a microbial population to utilize a contaminant as an energy source through the incorporation of carbons to form new biomass, and ultimately mineralize a contaminant to water and oxygen.

There are many different processes that occur during the transformation of a contaminant by a microbial population. In aerobic biodegradation, oxygen is used as an electron acceptor, while in anaerobic biodegradation, nitrate, sulfate, iron, manganese, carbon dioxide, and even the contaminant itself (during fermentation) are used as electron acceptors.[15] Some microbes are only able to utilize a contaminant as a growth substrate until a certain metabolite is formed and then, due to a lack of necessary enzymes, it is no longer able to transform it further.[25] Co-metabolism is another possible process and occurs when a contaminant is transformed in the

presence of a growth-substrate through enzymes that are stimulated within the cell or released by cells during energy consumption.[26] These processes, either independently or combined, determine the ability of a microbe or microbial population to biodegrade a contaminant.

1.4.1 Transformation Limitations for PAHs

There are several limiting factors affecting the ability of PAHs to undergo transformation or biodegradation. First, the PAH must be able to interact with enzymes within the microbial cell, or those that are bound to the surface of the cell, that are responsible for degradation or co-metabolism.[27] This requires the PAH to be solubilized in the region near the cell. PAHs have a low solubility in water, with ranges from 0.00019 to 30 g m^{-3} at 25^{o}C (Appendix A.1), and a strong affinity to organic matter.[28] Because of these physical chemical properties, PAHs have limited bioavailability and are less likely to have access to a cell than other more polar and water-soluble contaminants.[27] Second, to enter the cell, a PAH has to undergo passive transport from the water surrounding the cell to the cell membrane.[27] Passive transport is driven by the concentration gradient between the outside and inside of the cell.[28] Low bioavailability results in a small concentration gradient and, therefore, the driving force behind the transport is small but still occurs.[27] Third, for the degradation of a PAH to be initiated, either through direct metabolism or co-metabolism, the necessary enzymes must be present and expressed, and is heavily dependent on the genetic composition of the cell.[27] Finally, after the expression of the necessary enzymes, ring-hydroxylating monooxygenases or dioxygenases are required to initiate the first oxidation step.[27] After the first step, continued enzymatic breakdown

of a PAH relies on the ability of the cell to form new, structurally-dependent enzymes to complete ring-cleavage and additional oxidation steps.

1.4.2 Enzymatic Processes for the Biodegradation or Co-metabolism of PAHs

Bacteria contain highly diverse and selective oxygenases or hydroxylases that are utilized during aerobic metabolic processes (biodegradation).[11] An example of these reactions is shown in Figure 1.1. The initial step in the metabolic degradation of PAHs requires ring-hydroxylating oxygenases (RHOs), either as monooxygenases (RHMs) or dioxygenases (RHDs), during which one or two hydroxyl groups are introduced at regiospecific and stereoselective carbon atoms (Figure 1.1).[11] When a dioxygenase is used, either a cis- or trans-dihydrodiol is formed. The selection of the activation site is determined by the shape of the enzyme that influences the orientation of the PAH and the accessibility to carbons to undergo hydroxylation.[29,30] Different dihydrodiols may be formed depending on RHDs available within bacteria and these starting products determine the resulting metabolic pathway. [29,30]

After the PAH is hydroxylated, another important class of oxygenases, ring cleavage dioxygenases (RCD), is required for PAH degradation (Figure 1.1).[11] Dihydrodiols (like those discussed above) undergo dehydrogenation to form PAH-diols using dihydrodiols dehydrogenases (DHDGs).[11] RCDs, more specifically either meta- or ortho-cleavage (RCD1 or RCD 2), interact with PAH-diols and open the ring forming ring cleavage products based on the type of dioxygenase and structure of the PAH-diol. Further degradation of these products is a result of the presence of additional dehydrogenases eventually forming one of two types of ring cleavage

intermediates: salicylate-type or phthalate-type. Each of these types has several break-down pathways depending on the enzymes available.

Co-metabolism of PAHs occurs through the broad specificity of RHOs. *Pseudomonas* sp. NCIB 9816 contains a naphthalene dioxygenase that hydroxylates 50 aromatic compounds except for HMW PAHs.[31] *Pseudomonas aeruginosa* strain PAO1 encoded with plasmid NAH7 was able to express naphthalene dioxygenase genes capable of oxidizing acenaphthene, acenaphthylene, and fluorene.[32] *Sphingomonas* sp. strain LH128, with the dioxygenase complex, phnA1 fA2f, metabolizes phenanthrene and also oxidizes LMW PAHs, dibenzo-*p*-dioxin, and select HMW PAHs.[33] Similarly, *Sphingomonas* sp. strain CHY-1 utilizes RHD ht-PhnI to metabolize chrysene and initiates hydroxylation of LMW and HMW PAHs.[34] *Mycobacterium* sp. strain AP1 biomineralizes pyrene, phenanthrene, fluoranthene, and hexadecane, while also transforming acenaphthene, fluorene, and naphthalene, but not anthracene.[35] Each microbial species have different co-metabolism capabilities based on their RHOs.

Figure 1.1. Example of PAH oxidation by aerobic bacteria using phenanthrene from Mallick et al.[11]

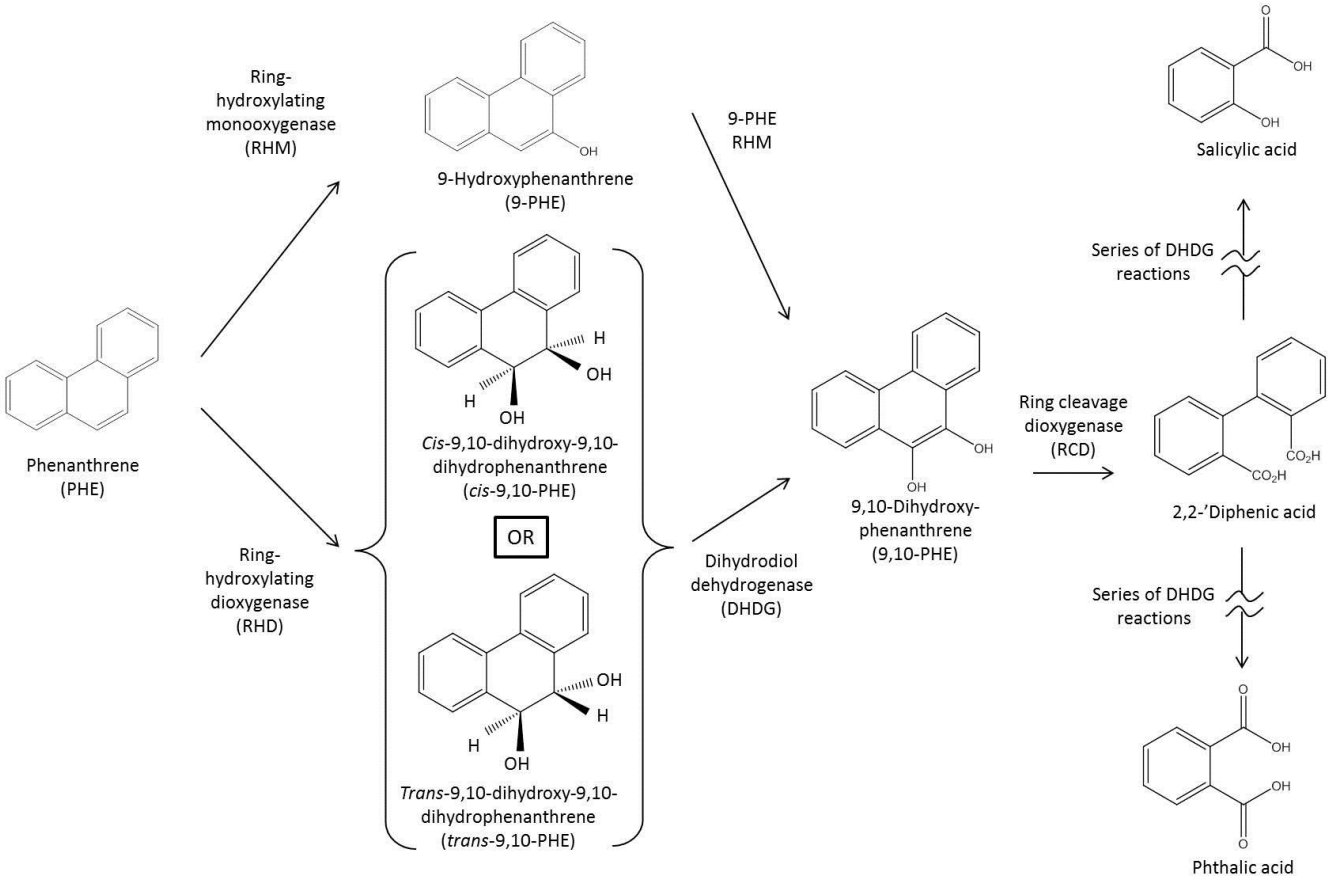

Variations of transformation rates during co-metabolism reactions are expected due to competitive interactions between the substrate and other PAHs with RHOs. For example, *Sphingomonas* sp. strain PheB4 utilizes phenanthrene as a sole carbon and energy source and co-metabolizes pyrene and fluoranthene.[36] The degradation of phenanthrene, and the formation of phenanthrene metabolites, were inhibited by the presence of both pyrene and fluoranthene, indicating the occurrence of competitive inhibition for substrate utilization. Competition between PAHs in mixtures for microbial enzymes is an important effect to consider because of the variations in transformation rates.

Growth substrates often promote the activation of different RHOs in microbes, which may not otherwise be present. *Mycobacterium* sp. strain 6PY1 has two RHDs, Pdo1 and Pdo2, responsible for the biomineralization of pyrene and phenanthrene.[37] Pdo1 is activated in cells grown on benzoate, phenanthrene, or pyrene, but not on acetate, while Pdo2 is only activated in cells grown on PAHs. The extensively researched PAH-biomineralizing *Mycobacterium* sp. strain PYR-1 has two RHO enzymes NidAB and NidA3B3.[38] Substrate specificity of NidAB did not show hydroxy, dihydrodiol, or dihydroxy metabolite formation, when exposed to toluene, *m*-xylene, phthalate, and biphenyl substrates. However, diol and dihydrodiol metabolites were formed when NidAB was incubated with dibenzothiophene, naphthalene, phenanthrene, and other LMW and HMW PAHs. Results for Nid A3B3 were similar, however benzyl alcohol was formed from toluene and 3-methylbenzyl alcohol was formed from m-xylene, as well as different isomers of PAH metabolites. *Mycobacterium aromativorans* JS19b1 cells grown in the presence of phenanthrene

contained phenanthrene degradation enzymes but these enzymes were not present in cells grown in nutrient broth and glucose.[39] Stimulation of certain RHOs may be possible in some microbes to increase transformation of specific contaminants.

Since substrate specificity promotes the activation of RHOs, and the structures of metabolites are determined by the RHOs that formed them, substrate specificity leads to the selectivity of metabolite formation.[40] Often, one isomer is produced in a higher ratio compared to other isomers. The RHD naphthalene 1,2-dioxygenase from *Pseudomonas* sp. NCIB 9816 formed (3S, 4R)-dihydroxy-3,4-dihydrophenanthrene with 90% selectivity from the co-metabolism of phenanthrene.[30] *Mycobacterium* sp. strain PYR-1, with enzyme NidA3B3, formed 3,4-, 9,10-, and 1,2-*cis*-dihydrodiol phenanthrene in a 2:1:1 ratio from phenanthrene.[41] RHOs determine the metabolite structure of the initial oxidation of the parent PAH.

In general, RHOs have a broad spectrum of PAH transformation capabilities and can be summarized by several properties.[40] First, one RHO has the ability to initiate oxidation on several different PAHs.[30,40] Second, the activity of RHOs varies depending on the PAH.[36,40] Third, different RHOs have different substrate specificities.[38,40] Classification of RHOs, based on these three properties, will enhance understanding behind biodegradation and co-metabolism capabilities.

1.4.3 Toxicity of PAH Metabolites

As mentioned previously, the extent to which bacteria are able to transform, biodegrade, or co-metabolize PAHs is dependent on the presence of specific enzymes present within the cell. Some bacteria are only able to degrade PAHs to a certain structure, causing an accumulation of PAH metabolites which may be more toxic than

the parent PAHs.[42-46] The toxicity of PAH metabolites have been evaluated after bioremediation of single PAHs.[46-48] Seedlings of sorghum and alfalfa were negatively affected by toxic phenanthrene degradation products formed by a rhizosphere microbe culture.[46] Mutagenicity of phenanthrene and its k-region (Appendix B1) derivatives was investigated using *Salmonella typhimurium* strains TA1535, TA 1537, TA1538, TA98, and TA100.[47] Phenanthrene showed no mutagenic potential but 9-hydroxyphenanthrene (9-PHE) and 9,10- mutagenic and 9,10-dihydroxyphenanthrene (9,10-PHE) and 9,10-phenanthrenequinone were both toxic and not mutagenic.[47] Other metabolites, such as *cis*- and *trans*-dihydroxy-9,10-dihydrophenanthrene, showed weak mutagenicity in only one of the *Salmonella* strains.[47] One study observed that a mixture of unidentified PAH metabolites formed during biodegradation of single PAHs, pyrene, fluoranthene, and phenanthrene, by *Mycobacterium* sp. SNP11 was less toxic compared to the parent PAHs.[48]

The toxicity of metabolites formed from bioremediation of two or more PAHs has also been studied.[45,49-51] For example, in bioremediated coal tar-contaminated soil from a manufactured gas plant, unknown PAH metabolites showed statically significant increases in developmental toxicity in zebrafish and in genotoxicity using the DT40 bioassay.[45] Toxicity studies involving PAH mixtures, and their metabolite mixture, have attempted to describe the toxicological result of a mixture in terms of an additive effect, the sum of the toxicity of the individual compounds, or antagonist effect (also referred to as sub-additive or subtractive), less than the expected toxicity if the effects were additive. Conclusions have been inconsistent and PAH mixtures produce both additive[51-54] and sub-additive[50,55-57] toxicological responses.

1.4.4 Transformation, Biodegradation, or Co-Metabolism of Phenanthrene

Many laboratory studies have used phenanthrene to study the ability for microbes to degrade PAHs. Phenanthrene is commonly described as a prototype PAH, due to the replication of its 3-ring structure throughout higher-ringed, more carcinogenic, PAHs such as benzo[a]pyrene.[58-60] Phenanthrene is also used a as a model PAH for metabolism studies because its bay-region and K-region (Figure B1) lead to the possible formation of more carcinogenic PAHs[47,61] in addition to modeling factors affecting microbial degradation (such as bioavailability and degradation potential).[58] Phenanthrene also has a moderate water solubility of 1.2 mg L^{-1} compared to larger PAHs with solubilities as low as 0.7 ng L^{-1} (benzo[k]fluoranthene) (Appendix A.1).

There have been many studies on phenanthrene alone, as well as part of PAH mixtures, using a wide variety of microbial populations. These studies include the use of unknown microbial consortia,[17,18,22,23,45,62-68] mixtures of several known microbial species,[60,63,69-71] and a single, known microbe species.[22,24,46,59,72-82]. Some strains capable of biomineralizing phenanthranene include *Acidovorax, Acinetobacter, Arthrobacter, Bacillus, Flavobacterium, Mycobacterium, Neptunomonas, Nocardia, Pseudomonas, Rhodococcus, Sphingomonas, Streptomyces,* and others.[59,83-85] Co-metabolism of phenanthrene has been seen in strains belonging to *Mycobacterium*,[10,35,41,86] *Pseudomonas*,[30] *Rhodococcus*,[10] and *Sphingomonas*.[33,34,36,77]

1.5 Co-metabolism of Phenanthrene by *Mycobacterium* sp. strain ELW1

This thesis is focused on the degradation of phenanthrene by *Mycobacterium* sp. strain ELW1 in aqueous systems. ELW1 was isolated from a stream sediment

sample cultured with isobutene (2-methylpropene) as the single source of carbon for growth and energy.[87] Classification of ELW is currently in progress by Michael Hyman at North Carolina State University but PCR sequencing of 16S RRNA genes from ELW1 showed similarities to *Mycobacterium sphagni* (GenBank accession number AB649002), *Mycobacterium* strain CP-2 (GenBank accession number AM056051), *Mycobacterium petroleophilum* ATCC 21497 (GenBank accession number AF480587), *Mycobacterium petroleophilum* ATCC 21498 (GenBank accession number), and *Mycobacterium* sp. strain TA27 (GenBank accession number AB028482). *Mycobacterium petroleiphilum*, and strain TA27, have known hydrocarbon-oxidizing activities.[88] While ELW1 successively grew on isobutene, studies showed growth on 1,2-epoxy-2-methylpropane and *cis*- and *trans*-2,3-epoxybutane. However, growth was not observed for other epoxides, C2 to C5 alkenes in straight-chain, branched, or chlorinated forms, or C1 to C6 n-alkanes, and others.[87] ELW1 uses a monooxygenase to initiate oxidation of 2-methylpropene at the double bond. The ability for ELW1 to degrade many types of contaminants, including PAHs, is currently unknown. The ability of ELW1 to utilize isobutene as a growth substrate has potential for the *in situ* stimulation of endogenous microbial populations through isobutene and oxygen addition. This may provide for a novel method to promote the initial oxidation of PAHs for subsurface bioremediation, through co-metabolic transformations.

1.6 Thesis Objectives

The potential for a novel microbe, *Mycobacterium* sp. strain ELW1, to transform phenanthrene in aqueous media was investigated. *Mycobacterium* sp. strain

ELW1 has genetic similarities to other *Mycobacterium* strains known to transform or biodegrade parent PAHs including 6PY1,[37] PYR-1,[38] SNP11,[48] TA27,[87,88] and *petroleiphilum*.[87,88] Therefore, the capability of ELW1 to transform PAHs was of interest. An aqueous system was used to optimize the bioavailability of phenanthrene and promote microbial degradation.[27]

The purpose of this study was to 1) determine the rate of phenanthrene transformation by ELW1, 2) identify phenanthrene metabolites and determine rates of formation for these metabolites by ELW1, 3) use Michaelis-Menten kinetics to model experimental data, and 4) characterize the toxicity of phenanthrene metabolites formed by ELW1.

CHAPTER 2.

TRANSFORMATION OF PHENANTHRENE BY MYCOBACTERIUM SP. ELW1 AND THE FORMATION OF TOXIC METABOLITES

Jill E. Schrlau,[1] Amber Kramer,[2] Anna Chlebowski,[3] Staci L. Massey Simonich,[2,3] and Lewis Semprini[1]

[1]Department of Chemical, Biological, and Environmental Engineering, Oregon State University, Corvallis, OR

[2]Department of Chemistry, Oregon State University, Corvallis, OR

[3]Department of Environmental and Molecular Toxicology, Oregon State University, Corvallis, OR

Contributions – Prepared by Jill E. Schrlau with editorial comments from Staci L. Massey Simonich and Lewis Semprini. Significant assistance with experiments and sample processing was provided by Amber Kramer. Zebrafish testing and advice was provided by Anna Chlebowski.

Manuscript prepared in preparation for submission to peer-reviewed journal, Environmental Science and Technology.

2.1 Abstract

Mycobacterium sp. ELW1 was able to co-metabolize phenanthrene (PHE) concentrations within its water solubility limit (~2 µmol) by ~48 hours. Hydroxyphenanthrene (OHPHE) metabolites were identified, including 1-hydroxyphenanthrene (1-PHE), 3-hydroxyphenanthrene (3-PHE), 4-hydroxyphenanthrene (4-PHE), 9-hydroxyphenanthrene (9-PHE), 9,10-dihydroxyphenanthrene (1,9-PHE), and *trans*-9,10-dihydroxy-9,10-dihydrophenanthrene (*trans*-9,10-PHE), and quantified over time. PHE transformation followed first-order kinetics, as well as Michael-Menten kinetics. Experimentally-determined ratio of the maximum rate of substrate utilization (k_{max}) and half-saturation concentration (K_S), (k_{max}/K_s), ranged 0.0019 – 0.0062 and estimated k_{max}/K_s ranged 0.0012-0.0024. Individual OHPHE standards, including 1-PHE, 3-PHE, 4-PHE, 9-PHE, and 1,9-PHE, were toxic to embryonic zebrafish (*Danio rerio*) with effective concentrations (EC_{50}) ranging 0.5-5.5 µM. PHE and *trans*-9,10-PHE were not toxic to embryonic zebrafish. PHE metabolite mixtures formed by ELW1 were tested on embryonic zebrafish in a range of concentrations. At the highest mixture concentration tested, OHPHE concentrations were at least 1.5 times less than the necessary concentration needed to elicit a toxic response based on the EC_{50}s from the OHPHE standards. However, a toxic response was observed for PHE-exposed cells at 76 and 122 hr. The contribution of the toxic metabolites to the mixture was similar between collections for both PHE-exposed cells and enzyme-inhibited cell controls (1-octyne controls). Therefore, the toxic response observed in OHPHE mixtures formed at 76 and 122 hr after ELW1 was exposed to PHE may have possibly been a caused by an unidentified toxic metabolite.

2.2 Introduction

Polycyclic aromatic hydrocarbons (PAHs) are compounds comprised of two or more fused benzene rings that form during the incomplete combustion of organic substances from both natural and anthropogenic sources.[1] PAHs are found in asphalt,[2] crude oil,[3] coal tar,[4-6] and creosote.[7,8] Many PAHs are considered to be probable or possible human and animal carcinogens by the International Agency for Research on Cancer (IARC) and also probable human carcinogens by the U.S. EPA Integrated Risk Information System.[9,12] Due to their ubiquity and known toxicity, remediation of PAH-contaminated systems is ongoing.

Bioremediation is a useful remediation technology because there are many strategies, specifically for aerobic systems, including the use of naturally-occurring microbial populations, biostimulation, and bioaugmentation *in situ* and/or *ex situ*. Plant-based compost and slow release fertilizers were used as a biostimulant in PAH contaminated soil which resulted in increased removal rates of PAHs and improved meiofauna diversity.[16-18,21] Biostimulated soil from an oil well contaminated with total petroleum hydrocarbons (TPHs) showed a 60% removal after 10 weeks.[24] Bioaugmentation was performed in a comparative study by Festa *et al*. where soil was spiked with phenanthrene (PHE), a 3-ringed parent PAH, and was bioaugmented with a bacterial consortium, as well as with an isolated *Sphingobuim* sp. strain.[23] Within 7 days, *Sphingobuim* sp. was able to degrade 75% of PHE and the bacterial consortium only removed 58%.[22] PHE was completely removed in the soils after 63 days in the by both *Sphingobuim* sp. and the bacterial consortium. [23] The combination of both biostimulation and bioaugmentation on PAH removal has also been studied.[17]

During bioremediation of PAHs, potentially toxic metabolites many be formed. Some bacteria are only able to degrade PAHs to a certain structure, causing an accumulation of PAH metabolites which may be more toxic than the parent PAHs.[42-45] Toxicity of PAH metabolites has been evaluated using a variety of studies.[45,49,72,89] Other studies have found that parent PAH compounds undergo detoxification through biodegradation as observed with *Mycobacterium* sp. SNP11 degradation of pyrene, fluoranthene, phenanthrene, and PAH metabolites.[48]

PHE has been frequently used to study the ability for microbes to degrade PAHs. PHE is commonly described as a prototype PAH, due to the replication of its 3-ring structure throughout higher-ringed, more carcinogenic, PAHs such as benzo[a]pyrene.[58-60] PHE is also used a as a model PAH for metabolism studies because its bay-region and K-region (Figure B1) lead to the possible formation of more carcinogenic PAHs,[47,61] in addition to modeling factors affecting microbial degradation (such as bioavailability and degradation potential).[58] PHE also has a moderate water solubility of 1.2 mg L^{-1} compared to larger PAHs with water solubilities as low as 0.7 ng L^{-1} (benzo[k]fluoranthene) (Appendix A.1).

There have been many studies on PHE alone, as well as part of PAH mixtures, using a wide variety of microbial populations. These studies include the use of unknown microbial consortia,[17,18,22,23,45,62-68] mixtures of several known microbial species,[60,63,69-71] and a single, known microbe species.[22,24,46,59,72-82] Examples of strains capable of biomineralizing PHE include *Mycobacterium*, *Pseudomonas*, *Rhodococcus*, *Sphingomonas*, and *Streptomyces*.[59,83-85] Co-metabolism of PHE has

been seen in strains belonging to *Mycobacterium,*[10,35,41,86] *Pseudomonas,*[30] *Rhodococcus,*[10] and *Sphingomonas.*[33,34,36,77]

The microorganism investigated in this study was *Mycobacterium* sp. strain ELW1 which was isolated from a stream sediment sample cultured with isobutene (2-methylpropene) as the single source of carbon for growth and energy.[87] Classification of ELW1 is currently in progress but PCR sequencing of 16S RRNA genes from ELW1 showed similarities to *Mycobacterium sphagni*, *M.*strain CP-2, *M. petroleophilum* ATCC 21497, *M. petroleophilum* ATCC 21498, and *M.* sp. strain TA27. *Mycobacterium petroleiphilum,* and strain TA27 have known hydrocarbon-oxidizing activities.[88] ELW1 is able to utilize isobutene as a carbon and energy source, with initial oxidization likely occurring as an epoxide. The ability of ELW1 to utilize isobutene as a growth substrate has potential for the *in situ* stimulation of endogenous microbial populations through isobutene and oxygen addition, and may lead to a novel method to promote the initial oxidation of PAHs for subsurface bioremediation, through co-metabolic transformations. The ability for ELW1 to degrade many types of contaminants, including PAHs, is currently unknown.

The purpose of this study was to determine the rate of PHE degradation by ELW1, identify PHE metabolites and determine rates of formation for these metabolites by ELW1, model experimental data using Michaelis-Menten kinetics, and characterize the toxicity of PHE metabolites formed by ELW1.

2.3. Materials and Methods

2.3.1 *Mycobacterium* sp. strain ELW1

2.3.1.1 Maintaining Microbial Culture

Pure *Mycobacterium* sp. strain ELW1 was originally isolated by, and acquired from, Michael Hyman at North Carolina State University.[87] The composition of mineral salt medium (MSM) has been previously described and is also provided in Appendix A.[87] For all experiments, batch cultures were started from plated cultures grown in the presence of isobutene and grown in 500 mL glass media bottles (Kimax Media Bottles, Kimble Chase, #61110-500) containing 303 mL MSM (Appendix A). Isobutene (~10% headspace (v/v)) was added to the batch culture every three days until the cell density was $OD_{600} > 0.7$, usually 6-8 days, using UV-VIS spectrophotometer analysis (Orion Aquamate 8000, ThermoFisher Scientific). Detailed methods regarding maintenance of culture purity is described in Appendix A.

2.3.2 Phenanthrene Transformation and Metabolite Formation Experiments

Cells grown in batch culture for 6-8 days were harvested, centrifuged, and re-suspended with fresh MSM. Activity of the concentrated cells was determined by measuring the rate of isobutene consumption. The method for activity tests, as well as the rates of isobutene consumption, is found in Appendix A and in Appendix A.9 and Appendix A.10. PHE standards were prepared in MeOH and spiked in 303 mL MSM in 500 mL media bottles at a maximum of 0.0089% MeOH (v/v) in each reactor, which did not negatively impact the activity of ELW1 (Appendix A.6). PHE-exposed cells were exposed to six different PHE masses, including 0.033, 0.068, 0.42, 0.84,

1.2, and 1.8 µmol, until PHE was no longer measured (see Section 2.3.3). In order to inhibit the monooxygenase enzyme involved in isobutene oxidation, gas-phase 1-octyne was added.[87] Cells exposed to PHE and 1-octyne aqueous concentrations of 11 µM 1-octyne (referred to as 1-octyne controls) were prepared by spiking 11 mL of a 1 mM stock gas-phase 1-octyne into the head space of the reactors containing cells. Preparation of the stock gas-phase 1-octyne is described in Appendix A and followed a previously published method.[90] The 1-octyne aqueous concentration of 11 µM was selected after measuring isobutene consumption of ELW1 in the presence of different 1-octyne aqueous concentrations and is described in Appendix A, Appendix A.7 and Appendix A.8. 1-Octyne controls were prepared with four different initial PHE masses, including 0.033, 0.068, 0.14, and 0.84 µmol. Additional controls included PHE-only reactors (MSM and PHE only) and cell-only reactors (MSM and cells only). All reactors were prepared in triplicate and MSM was equilibrated with isobutene and 1-ocytne (for 1-octyne controls) for ~1 hr prior to the addition of cells and PHE. Reactors were kept in a temperature-controlled (30^{o}C) room on a rotary shaker table at 200 rpm. Re-suspended cells were added to each reactor and the total cell protein (mg protein) per reactor was calculated using the protein assay described in Appendix A. Liquid samples were collected immediately after the addition of cells, followed by collections at approximately 1, 3, 5, 10, 22, 48, and 72 h, as needed, until the PHE mass in the samples was no longer measured using the method described in Section 2.3.3. Time zero represents the time in which the cells were lysed from exposure to organic solvents during the SPE extraction method (Section 2.3.3) and not the time in which an aliquot of the aqueous media was collected from

the reactor. The time between collection and cell lysing was ~1 - 1.5 hr, resulting in the concentration of PHE measured at time zero to be 74-99% of the PHE concentration initially spiked (Figure 2.1).

2.3.3 Analytical Method for the Measurement of Phenanthrene and OHPAH Metabolites

2.3.3.1 Extraction Method

PHE transformation samples (5 - 15 mL) from each of the 3 replicate batch reactors were spiked with labeled surrogates, listed in Appendix A.2, immediately after collection to account for analyte loss during sample processing. Toxicology samples were not spiked with surrogates since labeled standards will affect the overall toxicity. All samples were extracted using solid phase extraction (SPE) with Bond Elut Plexa (30 mg, 3 mL) cartridges (Agilent Technologies, New Castle, DE) following a modified version of a previously published method and described in detail in Appendix A.[91] After SPE, PHE transformation sample extracts were solvent exchanged to ethyl acetate and spiked with an internal standard for a final volume of 300 µL. Toxicology extracts were split gravimetrically with 80% of the extract used for toxicology testing (toxicology fractions) and the remaining 20% used for chemical analysis (chemical fractions). Compounds concentrations measured in the chemical fractions were used to estimate the concentrations present in toxicological fractions. The toxicology fractions were blown to dryness and reconstituted with 100 µL dimethyl sulfoxide (DMSO) (Sigma Aldrich, St. Louis, MO) to a concentration of ~8 mM PHE-equivalent. The chemical fractions were solvent exchanged to ethyl acetate and spiked with labeled surrogates and internal standards (Appendix A.3) for a final volume of 300 µL and analyzed for PHE. Extracts were further processed in

preparation for OHPHE analysis (described below). Recovery of PHE across the method was 54 ± 2.7% (Appendix A.2).

In addition to PHE analysis, all extracts were analyzed for OHPAHs. Briefly, 50 µL of the 300 µL sample extract was transferred into a 300 µL spring insert containing 100 µL acetonitrile and 20 µL toluene and concentrated to 20 µL using a fine stream of nitrogen.[91,92] The derivatization reagent, N,O-bis-(trimethylsilyl) trifluoroacetamide (BSTFA), was added to the extract (30 µL), the mixture was incubated at 70 ^{o}C for 40 min, and analyzed with the instrumental method described in Section 2.3.3.3.[92] Storage stability of OHPAHs, as well as intra- and inter-day variability, has been previously assessed.[91] The percent change observed in storage stability was up to 10% and for intra- and inter-day variability was 2-5%.[91] OHPHE recovery across the method used in this study ranged from 19 ± 1.5 – 92 ± 16% (Appendix A.2).

2.3.3.2 Gas Chromatography Mass Spectrometry (GC/MS) Analysis of Phenanthrene

PHE was analyzed on an Agilent 6890 gas chromatograph (GC) coupled to a 5973N mass spectrometer (MS) with electron impact (EI) ionization in selective ion monitoring (SIM) mode. A DB-5MS (Agilent, 30 m × 0.25 mm I.D., 0.25 µm film thickness) column was used with a constant flow of helium at 0.9 mL min^{-1}. The inlet was operated in splitless mode and the inlet and interface temperatures were maintained at 300^{o}C. The oven temperature program began at 60 ^{o}C, held 1 min, ramped at 7.5 ^{o}C min^{-1} until 220 ^{o}C, ramped at 110 ^{o}C min^{-1} until 320 ^{o}C, and held for 5 min for a total run time of 28.24 min. The ion source and quadrupole were set to 230 ^{o}C and 150 ^{o}C, respectively. The estimated detection limits (EDLs) were

calculated following EPA Method 8280 and was 0.51 pg μL^{-1} for PHE (Appendix A.2).[93]

2.3.3.3 GC/MS Analysis of OHPAHs

OHPAHs were analyzed in both SIM and full scan modes using the same instrumentation described above. For SIM, commercially available standards were used to quantify OHPAHs that were able to be derivatized by BSTFA. SIM method parameters for BSTFA-derivatized OHPAHs, including windows, fragmentation ions, and retention times, are listed in Appendix A.2. Fragmentation ions were predicted according to a previously-described method and described in SI.[92] A DB-5MS column was used constant flow of 1 mL min^{-1} of He and a constant inlet temperature of 280 ^{o}C in splitless mode. The oven temperature program was as follows: 70 ^{o}C for 1 min, ramp at 15 ^{o}C min^{-1} until 200 ^{o}C, hold for 5 min, ramp at 10 ^{o}C min^{-1} until 320 ^{o}C, and hold for 1 min for total run time of 27.67 min. The interface temperature was 280 ^{o}C. Using this method, *cis*-9,10-PHE and *trans*-9,10-PHE co-eluted. To separate these two isomers, the following oven temperature program was used (all other method parameters remained the same): 70 ^{o}C for 1 min, ramp at 2 ^{o}C min^{-1} until 320 ^{o}C, and hold for 1 min for a total run time of 127 min. The EDLs for all OHPAHs ranged 0.32 – 5.0 pg μL^{-1} (Appendix A.2).

2.3.4 Co-metabolism Kinetics for Phenanthrene Transformation by ELW1

2.3.4.1 Zero-order and First-order Rates of Transformation and Rates of Formation

Zero-order transformation rates of PHE and formation rates of metabolites were determined from a three-point linear regression within the first six hours after cells were exposed to PHE for each PHE mass tested. The mass balances for PHE-

exposed cells at 0.068, 1.2, and 1.8 µmol, and for 1-octyne-inhibited controls at 0.068, 0.14, and 0.84 µmol, were evaluated by summing the zero-order OHPHE metabolite formation rates and compared to the zero-order transformation rates of PHE. PHE transformation by ELW1 was also described by first-order rates and these rate constants were obtained by fitting a linear regression model to natural log-transformed aqueous concentrations of PHE measured within the first six hours after cells were exposed to PHE. First-order rate constants were normalized by biomass (in terms of mg protein) to compare non-normalized and normalized rates and also to determine the ratio of k_{max} and K_S at each PHE mass tested (see Section 2.3.4.2).

2.3.4.2 Modeling Enzyme Kinetics

The enzyme kinetics for the co-metabolism of PHE was modeled using experimentally-determined PHE transformation rates and the modified Michaelis-Menten equation:[94]

$$\frac{dC_{aq,PHE}}{dt} = \frac{k_{max}C_{aq,PHE}}{K_S + C_{aq,PHE}} \quad (2.1)$$

where $C_{aq,PHE}$ is the aqueous concentration of PHE (µM), t is time (hr), k_{max} is the maximum rate of PHE transformation normalized to biomass (µmol mg^{-1} $protein^{-1}$ hr^{-1}), and K_S is the concentration of PHE transformed at half of the maximum rate of transformation (µM). Due to the water solubility limit of PHE, k_{max} and K_S could not be determined experimentally. Therefore, k_{max} and K_S were estimated using a non-linear method (generated two different sets of k_{max} and K_S) and a linearization method (generated one set of k_{max} and K_S) to obtain three sets of k_{max} and K_S estimates. The three sets of k_{max} and K_S were as follows: 1) a non-linear method involving least-squared residual analysis between the zero-order PHE transformation rate at each

PHE concentration obtained experimentally and the Michaelis-Menten model (equation 2.1) predicted rate using Excel's Solver utility (2016) to solve for both variables simultaneously (Model 1); 2) same as the previous method but k_{max} was set to the solubility limit of PHE (6.7 µM) and Solver was used to estimate K_S (Model 2); and 3) linearization of experimental data using the Lineweaver-Burk plot (Model 3). Experimental values of k_{max}/K_S are equivalent to biomass-normalized first-order PHE transformation rates.

2.3.5 Toxicity of OHPHE metabolites

2.3.5.1 Embryonic Zebrafish Bioassay

Embryonic zebrafish were exposed to individual OHPAH standards and to OHPAH metabolite mixtures formed by ELW1 (toxicology fractions described in Section 2.3.3.1) following the method described in Truong *et al*.[95] In brief, at 6 hours post-fertilization (hpf), dechorinated zebrafish (n = 32) embryos were exposed to different concentrations of either OHPAH standards or mixtures of metabolites produced by ELW1 (toxicology fractions). Embryonic zebrafish were evaluated for mortality and developmental effects at 24 hpf and larval morphology and behavioral endpoints at 120 hpf. Significant differences in responses for control and exposed embryonic zebrafish were evaluated using Fisher's Exact test.[96]

2.3.5.2 Cell Viability During PHE Exposure

Cell viability tests were performed on PHE-exposed cells (0.42, 0.84, and 1.8 µmol), 1-octyne controls (0.84 µmol), and cells-only controls using Live/Dead cell staining and flow cytometry as described in Appendix A. Aliquots of 50, 100, or 250 µL were removed from the batch reactors over time and diluted to 0.5 mL with ultra-

pure deionized water, followed by the addition of 0.5 µL of fluorescent dye to achieve ~10,000 events μL^{-1}. The cells were incubated in the presence of the dye for 20 mins and analyzed on the flow cytometer (Appendix A).

2.3.6 Statistical Analyses

Statistical analyses were performed using JMP 12 software (by SAS). Differences between triplicate means for both zero-order and first-order rate constants were evaluated using Student t-tests with statistical significance resulting in a p-value ≤ 0.05.

2.4. Results and Discussion

2.4.1 Phenanthrene Transformation and Metabolite Formation by ELW1

PHE was completely co-metabolically transformed by PHE-exposed cells within 29 hr at initial PHE masses of 0.033, 0.068, 0.42, 0.84, and 1.8 µmol and within 47 hrs for 1.2 µmol (Figure 2.1A). The activity of the pre-exposed cells, determined by the rate of isobutene consumption, used in all PHE transformation experiments were statistically similar (Appendix A.9 and Appendix A.10). Therefore, the longer time required for PHE transformation in the cells exposed to 1.2 µmol PHE was not due to decreased activity of the cells. In the 1-octyne controls, 26-49% of PHE was transformed at the final time point (Figure 2.1B). In the PHE-only controls, 6-31% of PHE was lost throughout the experimental period, suggesting that adsorption to the reactor walls had occurred (Figure 2.1C). Taking into account the loss of PHE to adsorption, 1-octyne effectively, but not completely, inhibited alkene monooxygenases used to initiate oxidation of aromatic rings (Figure 2.1B).[87]

Figure 2.1. Transformation of six PHE masses (with standard error bars, $n = 3$ except for 1-octyne control exposed to 0.84 µmol PHE, $n = 2$) by ELW1 for PHE-exposed cells (solid lines) (A), 1-octyne controls (dashed lines) (B), and PHE-only control (dotted lines) (C).

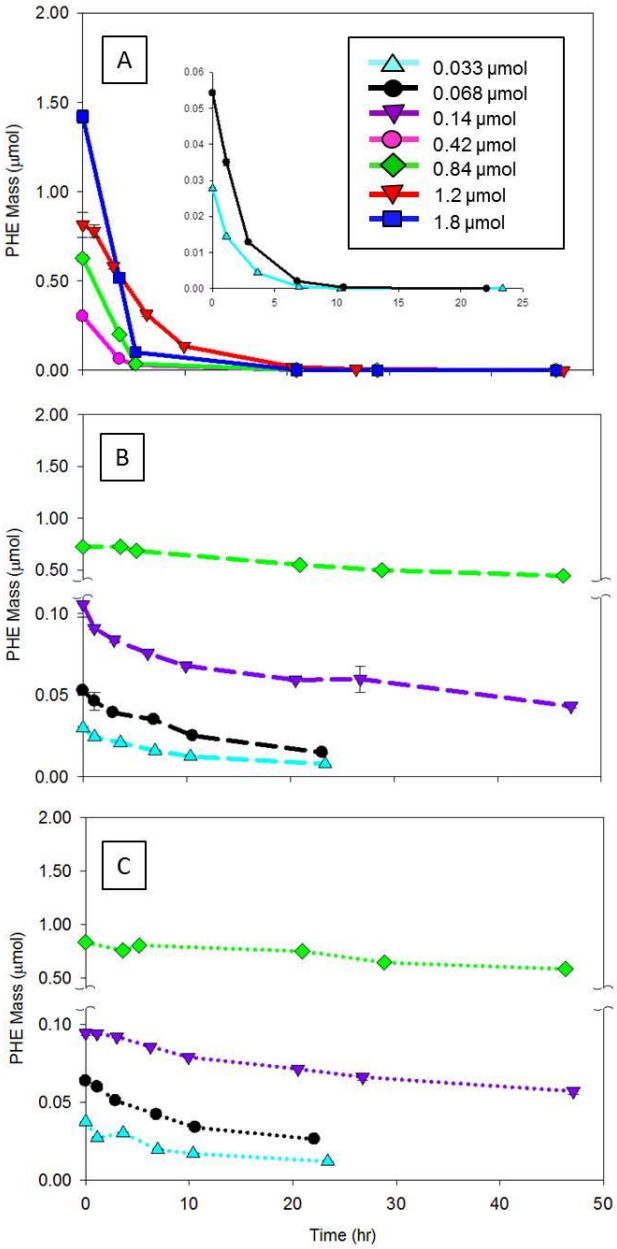

Samples collected from PHE-exposed cells, 1-octyne controls, PHE-only controls, and cells-only controls batch reactors were analyzed for 16 commercially-available OHPAH metabolites (Appendix A.4) at three different initial PHE masses (Figure 2.2 and Figure 2.3). While OHPHE metabolites were measured in both the

PHE-exposed cells (Figure 2.2) and 1-octyne controls (Figure 2.3), including 1-PHE, 3-PHE, 4-PHE, 9-PHE, 1,9-PHE, and *trans*-9,10-PHE, the concentrations in the PHE-exposed cells were significantly higher than the 1-octyne control for 0.068 µmol, which was the only PHE mass tested in both reactors. The remaining OHPHE metabolites, 2-PHE, *cis*-9,10-PHE, and other OHPAHs on our analyte list (Appendix A.4) were not detected. The primary OHPHE metabolite formed by both PHE-exposed cells and 1-octyne controls at all PHE masses was *trans*-9,10-PHE, with percent contributions to the total mass of OHPHE metabolite ranging 92-99% and 72-100%, respectively. In both cases, the *trans*-9,10-PHE was formed as PHE was transformed and remained constant at a concentration maximum for the duration of each experiment (Figure 2.2 and Figure 2.3, respectively). OHPAH metabolites were not detected in the PHE-only or cells-only controls.

Several studies have identified PHE metabolites during degradation and cometabolism by other microorganisms. According to the summary of PHE degradation pathways presented in Mallick *et al*, both *trans*-9,10-PHE and *cis*-9,10-PHE are possible products resulting from the initial oxidation of the 9 and 10 positions during PHE metabolism [11]. The *trans*-9,10-PHE isomer, formed from an epoxide at the 9,10 position (9,10-epoxy-9,10-dihydroxyphenanthrene), is a dead-end product but *cis*-9,10-PHE may be further oxidized to form 9,10-PHE.[11] *Trans*-9,10-PHE was the sole metabolite formed during cometabolism of PHE by *Mycobacterium*

Figure 2.2. Transformation of PHE and formation of OHPHE metabolites (with standard error bars, $n = 3$) by PHE-exposed cells for initial PHE masses of 0.068 µmol (A and B), 1.2 µmol (C and D), and 1.8 µmol (E and F). Note that the y-axes scales are different in each plot.

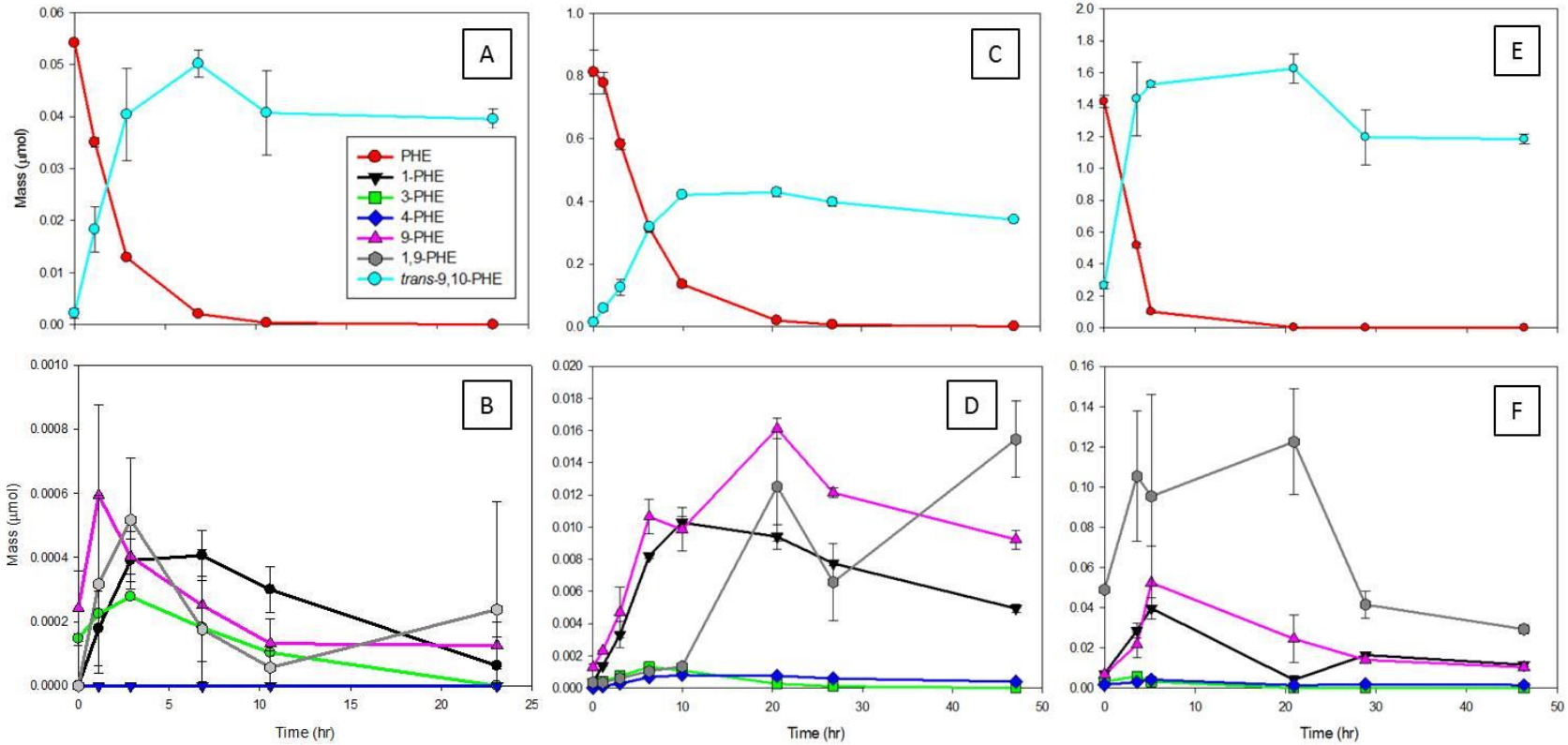

Figure 2.3. Transformation of PHE and formation of OHPHE metabolites (with standard error bars, $n = 3$ except for 0.84 µmol PHE, $n = 2$) by 1-octyne controls for initial PHE concentrations of 0.068 µmol (A and B), 0.14 µmol (C and D), and 0.84 µmol (E and F). Note that the y-axes scales are different ineach plot.

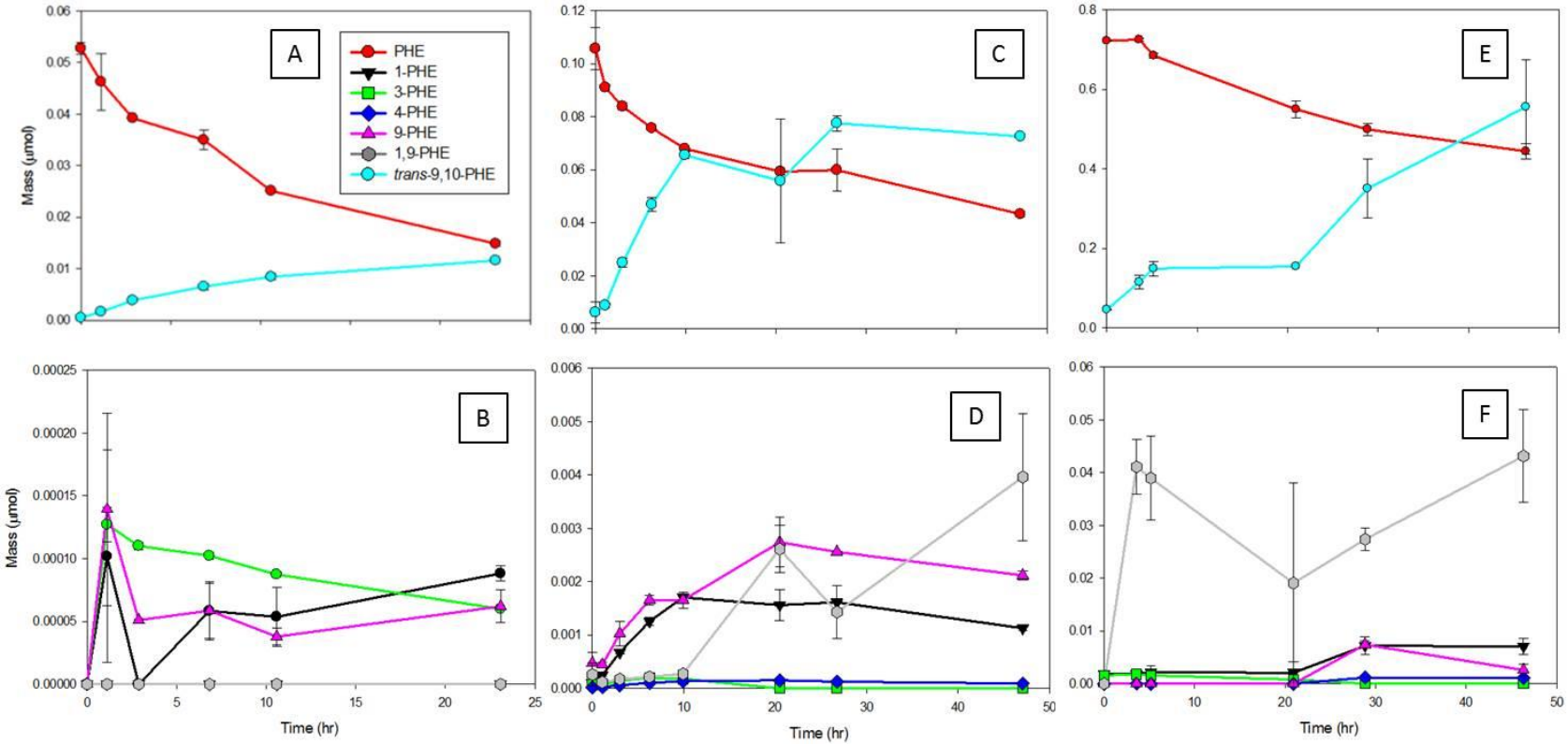

strain S1 grown in the presence of anthracene.[74] The absence of *cis*-9,10-PHE in the current study was confirmed with authentic standards. However, the formation of *cis*-dihydrodiols, including *cis*-3,4-PHE (*Mycobacterium* sp. strain 6PY1, *M. vanbaalenii* strain PYR-1, and *Sphingomonas* sp. strain A4),[37,38,41,97] *cis*-9,10-PHE (*M. aromativorans* JS19b1),[38,41,82,98] and *cis*-1,2-PHE (*M. aromativorans* JS19b1),[41,82] have been previously measured. Kim *et al* also measured additional OHPHE metabolites including 2- and 3-PHE, 9,10-PHE, and one additional phenanthrenediol.[41] Identification of other PHE metabolites structures further in PHE degradation pathways presented in Mallick *et al*,[11] including coumarins, benzocourmarins, and 1-OH-2-naphthoic acid, have also been made.[69,75,79,98] In this study, 1-OH-2-naphthoic acid was not detected, suggesting PHE cometabolism by ELW1 did not form *cis*-1,2-PHE or *cis*-3,4-PHE, or that ELW1 was not able to transform these products to 1-OH-2-naphthoic acid.[11] Based on the consistency of *trans*-9,10-PHE concentrations over time and its high contribution to the total mass of the OHPHE metabolites formed, *trans*-9,10-PHE did not appear to undergo further transformation in by ELW1.

The formation of 1-PHE, 9-PHE, and 1,9-PHE by ELW1 may occur through following several different pathways shown in Figure 2.4. Each oxidation step requires different enzymes, include ring hydroxylating monooxygenase (RHM), ring hydroxylating dioxygenases (RHD), dihydrodiol dehydrolase (DHDL), and enzymes capable of hydrolyzing one and two epoxides generally named epoxide monohydrolase (EML) and epoxide dihydrolase (EDL). Formation and accumulation of epoxides, specifically epoxyethane during the consumption of ethene, by ELW1

has been previously shown.[87] In addition, the presence of a gene responsible for encoding an epoxide hydrolase is located near to the genes that form the monoxygenase that oxidizes isobutene.[99] Both the epoxide hydrolase and isobutene-oxidizing monooxygenases are expressed at high levels in ELW1 grown on isobutene.[99] These epoxide-forming monooxygenases that initiated oxidation of alkenes were inhibited by 1-octyne.[87] Therefore, the formation of all the metabolites, particularly 1-PHE, 9-PHE, 1,9-PHE, and *trans*-9,10-PHE likely occur through epoxides. Additional experiments are needed to elucidate these pathways.

Figure 2.4. Possible formation pathways of 1-PHE, 9-PHE, and 1,9-PHE by ELW. Enzymes required to form oxidized structures are listed near the reaction arrow and include ring hydroxylating monooxygenase (RHM), ring hydroxylating dioxygenases (RHD), dihydrodiol dehydrolase (DHDL), epoxide monohydrolase (EML) and epoxide dihydrolase (EDL). Compounds in blue, and names bolded with an asterisk (*), represent those that were commercially-available and measured in this study.

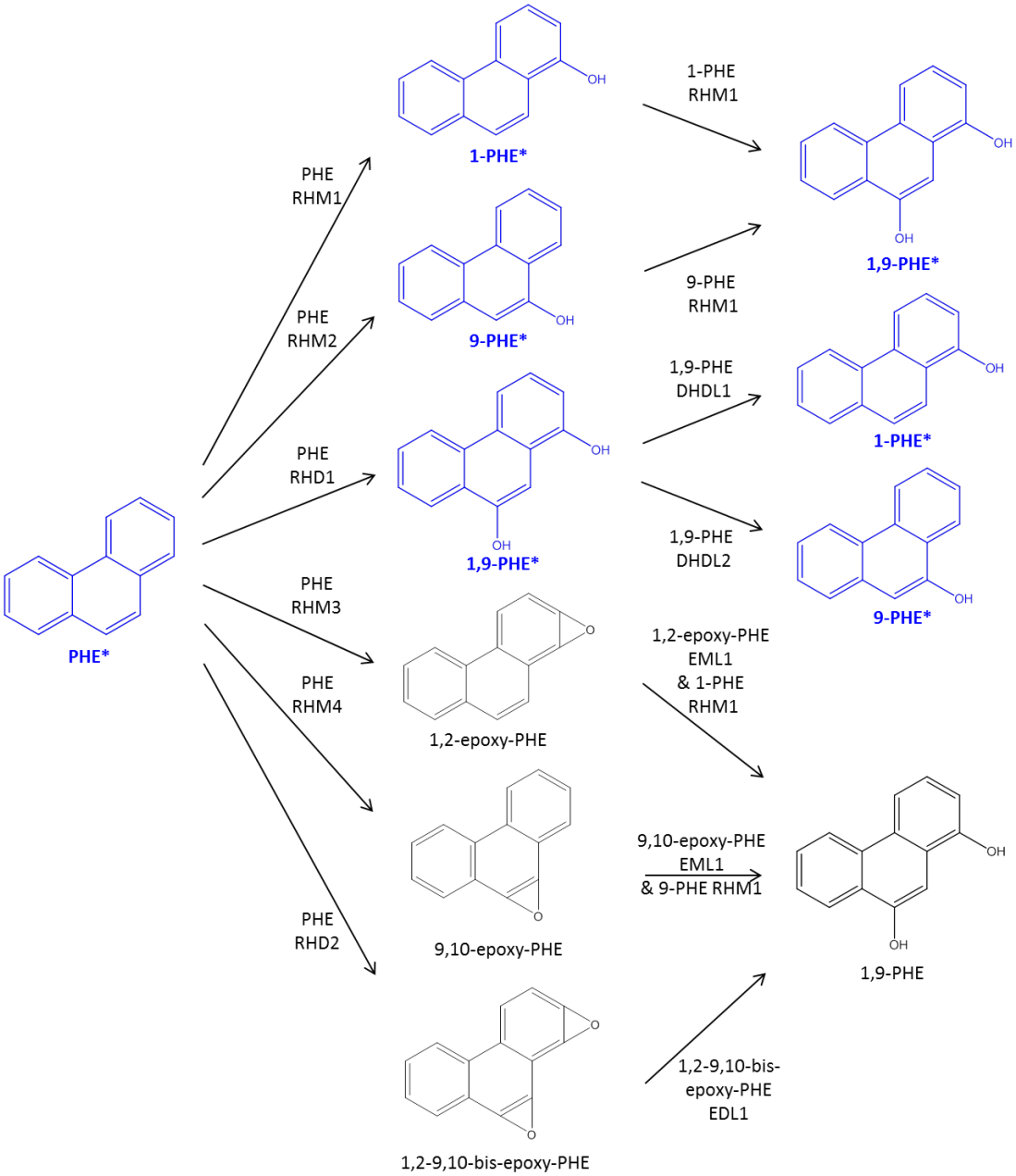

2.4.2 Co-Metabolism Kinetics for Phenanthrene Transformation by ELW1

2.4.2.1 Zero-order and First-order Rates of Transformation and Rates of Formation

Average biomass-normalized zero-order PHE transformation rates increased with increasing initial mass of PHE for PHE-exposed cells (Table 2.1). The transformation rates for PHE-exposed cells were significantly different (*p*-value < 0.01) for all PHE masses except for the rates at 0.033 and 0.068 µmol and at 0.42 and 0.84 µmol. In contrast, for 1-octyne controls, the zero-order PHE transformation rates were not statistically different for any of the PHE masses tested in the 1-octyne controls (*p*-value > 0.05). The significantly slower rates of PHE transformation by 1-octyne controls, compared to the PHE-exposed cells, further supports findings that the alkene monooxygenases capable of oxidizing PHE were successfully inhibited by 1-octyne.

Table 2.1 Average zero-order PHE transformation rates (with standard errors, $n = 3$ except for 1-octyne control exposed to 0.84 µmol PHE, $n = 2$) for all initial PHE masses. Rates were calculated from changes in PHE concentration in the six hours following ELW1 exposure to PHE. Transformation rates that were not statistically different (*p*-value > 0.05) are designated by the same superscript letter. NA: Not applicable - cells were not exposed to that PHE mass.

		PHE-Exposed Cells	1-Octyne-Inhibited Cells
PHE Mass (µmol)	ELW 1 Mass (mg protein)	k ± SE (fmol mg^{-1} $protein^{-1}$ hr^{-1})	k ± SE (fmol mg^{-1} $protein^{-1}$ hr^{-1})
0.033	25.6	1.3 ± 0.014^{A}	0.50 ± 0.028^{A}
0.068	26.2	2.4 ± 0.54^{A}	0.99 ± 0.10^{A}
0.14	25.4	NA	1.5 ± 0.51^{A}
0.42	40.4	7.8 ± 0.15^{B}	NA
0.84	40.4	11 ± 3.7^{B}	1.3 ± 0.12^{A}
1.2	25.4	20 ± 1.1^{C}	NA
1.8	40.4	35 ± 11^{D}	NA

In prior literature, zero-order PHE transformation rates were typically reported not normalized by biomass. The non-normalized PHE transformation rates for this study, 0.0060 – 0.25 μmol hr^{-1}, were in good agreement with other reported PHE rates by several *Mycobacterium* sp. strains, including A1-PYR (0.019 μmol hr^{-1})[69] and PYR-GCK, JS19b1, czh-3, and czh-117 (0.0020 – 0.019 μmol hr^{-1}).[98]

Average biomass-normalized zero-order rates of formation for OHPHE metabolites increased with increasing PHE mass for both PHE-exposed cells and 1-octyne controls (Table 2.2). Rates of formation for each OHPHE, in both PHE-exposed cells and 1-octyne controls, significantly increased (p-value < 0.04) as the initial PHE mass increased. Insignificant increases in zero-order formation rates between PHE masses for other OHPHE metabolites in PHE-exposed cells were likely due to the high variability in measured concentrations of derivatized OHPHE metabolites (Figure 2.2 and Table 2.2). Derivatization increases chromatographic noise due to the excess derivatizing agent present in the sample.[91] For several of the OHPHEs measured in the 1-octyne controls, zero-order rates could not be determined because of limitations due to instrumental detection limits and/or poor chromatography (Table 2.2).

Table 2.2 Average biomass-normalized zero-order OHPHE metabolite formation rates (with standard errors, $n = 3$ except for 1-octyne control exposed to 0.84 µmol PHE, $n = 2$) for PHE-exposed cells and 1-octyne controls at different PHE masses. **Units for rates are fmol mg^{-1} protein^{-1} hr^{-1}.** ND: Not detected. NA: 3-point regression line was not available.

	PHE-Exposed Cells			1-octyne controls		
OHPHE Metabolite	0.068 µmol	1.2 µmol	1.8 µmol	0.068 µmol	0.14 µmol	0.84 µmol
1-PHE	0.0022 ± 0.0032	0.032 ± 0.00058	0.064 ± 0.015	NA	0.0047 ± 0.00030	NA
2-PHE	ND	ND	ND	ND	0.000023 ± 0.0000013	0.0039 ± 0.0000601
3-PHE	0.00072 ± 0.000034	0.0045 ± 0.00014	NA	NA	0.00057 ± 0.000030	NA
4-PHE	ND	0.0026 ± 0.000066	0.0043 ± 0.00054	ND	0.00037 ± 0.000011	NA
9-PHE	0.00060 ± 0.00020	0.031 ± 0.0055	0.073 ± 0.037	NA	0.0056 ± 0.00047	NA
1,9-PHE	NA	0.0036 ± 0.00089	0.058 ± 0.019	ND	0.00048 ± 0.00015	0.14 ± 0.018
trans-9,10-PHE	0.22 ± 0.024	1.3 ± 0.045	2.7 ± 0.99	0.024 ± 0.0018	0.17 ± 0.044	0.33 ± 0.043
Average Sum of Zero-order OHPHE Formation	0.22 ± 0.024	1.3 ± 0.047	2.9 ± 1.0	0.016 ± 0.0067	0.18 ± 0.0049	0.47 ± 0.050
Zero-order PHE Transformation	0.24 ± 0.054	2.0 ± 0.11	3.5 ± 0.11	0.099 ± 0.010	0.15 ± 0.051	0.13 ± 0.012
% Difference	7	32	17	83	-20	-254

Mass balances between PHE transformation and OHPHE formation were assessed for PHE-exposed cells and 1-octyne controls by taking the sum of OHPHE zero-order formation rates (Table 2.2) and comparing them to the zero-order rate of PHE transformation (Table 2.1). For PHE-exposed cells, the difference ranged from 7

- 32%, whereas for the 1-octyne-inhibted controls, differences ranged from 20-(-254)%. In biological systems, large variability is often observed.[100] Assuming up to 15% of variability can be attributed to OHPAH stability in storage,[91] in addition to 15% variability in biological systems,[100] it was assumed that mass balance was achieved when the differences between PHE transformation and OHPHE formation rates was ~ 30%. Thus, in the PHE-exposed cells, the transformation of PHE was essentially completely accounted for by the formation of OHPHE metabolites. In the 1-octyne controls, mass balance was achieved for 0.14 µmol, but not for the other experiments. These findings could be explained by either the metabolites formed at concentrations below the instrumental detection limits (0.068 µmol) or metabolite concentrations were over-estimated during the analysis of the derivatized samples (0.84 µmol). Abiotic losses, and their rates, were not accounted for in this comparison.

PHE transformation by ELW followed first-order kinetics (Appendix A.11). First-order rates, k_{PHE}, and half-lives, $t_{1/2}$, for PHE-exposed cells ranged 0.16 – 0.51 hr^{-1} and 1.4 - 4.3 hr, respectively, and the 1-octyne controls ranged 0.015 – 0.10 hr^{-1} and 7.0 - 47 hr, respectively (Table 2.2). Similar to zero-order rates, k_{PHE} for the 1-octyne controls were significantly slower compared to PHE-exposed cells. The k_{PHE} and $t_{1/2}$ for PHE-exposed cells were statistically similar, except for 1.2 µmol, which had a k_{PHE} significantly lower and a $t_{1/2}$ significantly higher than those at other PHE masses (*p*-value <0.0001). For 1-octyne controls, k_{PHE} and $t_{1/2}$ for 0.14 and 0.84 µmol were statistically different than the lower PHE masses (*p*-value <0.003). Normalizing

the first-order rates of PHE transformation by biomass, $k_{bio,PHE}$, did not account for these differences (Table 2.3).

The first-order rates of PHE transformation in this study were much faster than those previously reported for other microorganisms.[101] First-order rates for PHE transformation, as part of a mixture of fluoranthene and pyrene, by *Mycobacterium* sp. PYR-1 were 0.0015 hr^{-1}, and by *Pasteurella* spp. were 0.0005 hr^{-1}.[101] However, competitive inhibition between the PAHs and microbial enzymes may have contributed to the rate since the fluoranthene degradation declined in the presence of other PAHs compared to single PAH studies.[101] Biomass-normalized first-order transformation rates are discussed further in Section 2.4.2.2.

Table 2.3. Average first-order PHE transformation rates, k_{PHE} (hr^{-1}) with PHE half-lives, $t_{1/2}$ (hr) and biomass-normalized first-order PHE transformation rates, $k_{bio,PHE}$ (L mg^{-1} protein^{-1} hr^{-1}) with $t_{bio,1/2}$ (hr) (with standard error, SE, n = 3 except for 1-octyne-inhibted controls at 0.84 µmol where n = 2) for each PHE mass in the first six hours following ELW1 exposure to PHE. NA: Not applicable - cells were not exposed to that PHE mass. Values that were not statistically different are indicated by the same superscript letter.

		Non-Normalized by Biomass				Normalized by Biomass			
		PHE-Exposed Cells		1-Octyne Controls		PHE-Exposed Cells		1-Octyne Controls	
PHE Mass (µmol)	ELW1 Mass (mg)	k_{PHE} ± SE (hr^{-1})	$t_{1/2}$ ± SE (hr)	k_{PHE} ± SE (hr^{-1})	$t_{1/2}$ ± SE (hr)	$k_{bio,PHE}$ ± SE (L hr^{-1} mg^{-1} protein^{-1})	$t_{bio,1/2}$ ± SE* (hr)	$k_{bio,PHE}$ ± SE (L hr^{-1} mg^{-1} protein^{-1})	$t_{bio,1/2}$ ± SE* (hr)
0.033	25.6	0.50 ± 0.01 ^{A}	1.4 ± 0.02 ^{C}	0.092 ± 0.035 ^{E}	7.5 ± 0.27 ^{G}	0.0063 ± 0.00009 ^{J}	115 ± 1.8 ^{M}	0.0011 ± 0.00004 ^{P}	629 ± 23 ^{R}
0.068	26.2	0.50 ± 0.01 ^{A}	1.4 ± 0.04 ^{C}	0.10 ± 0.010 ^{E}	7.0 ± 0.72 ^{G}	0.0059 ± 0.0002 ^{J}	118 ± 3.184 ^{M}	0.0012 ± 0.00012 ^{P}	600 ± 61 ^{R}
0.14	25.4	NA	NA	0.035 ± 0.0021 ^{F}	20 ± 1.3 ^{H}	NA	NA	0.00042 ± 0.00003 ^{Q}	1675 ± 110 ^{R}
0.42	40.4	0.46 ± 0.03 ^{A}	1.5 ± 0.11 ^{C}	NA	NA	0.0035 ± 0.0002 ^{K}	203 ± 15 ^{N}	NA	NA
0.84	40.4	0.51 ± 0.20 ^{A}	1.4 ± 0.05 ^{C}	0.015 ± 0.002 ^{F}	47 ± 6.2 ^{I}	0.0039 ± 0.0002 ^{K}	180 ± 6.7 ^{N}	0.00012± 0.000015 ^{Q}	6208 ± 809 ^{S}
1.2	25.4	0.16 ± 0.01 ^{B}	4.3 ± 0.31 ^{D}	NA	NA	0.0019 ± 0.0001 ^{L}	360 ± 26 ^{O}	NA	NA
1.8	40.4	0.47 ± 0.02 ^{A}	1.5 ± 0.05 ^{C}	NA	NA	0.0036 ± 0.0001 ^{K}	193 ± 6.8 ^{N}	NA	NA

* Half-life per biomass concentration in mg protein L^{-1}.

2.4.2.2 Modeling Enzyme Kinetics

The enzyme kinetics of the co-metabolism of PHE was modeled using experimentally determined PHE transformation rates and values of k_{max} and K_S estimated using non-linear (Model 1 and 2) and linearization (Model 3) methods (described in Methods, Section 2.3.4.2). Models 1 and Model 2 showed a good fit to the experimental data for all points and Model 3 showed a good fit at lower PHE concentrations (μM), but deviated substantially from experimental data at higher PHE concentrations (Figure 2.5). The better fit of Model 1 and Model 2 indicated that k_{max} and K_S (Table 2.4) were more accurately estimated with non-linear methods. The poor fit for Model 3 resulted from the use of the Lineweaver-Burk plot to determine k_{max} and K_S (Appendix A.12 and Table 3.6), which can lead to estimate errors because the linear regression of the inverse values were strongly influenced by the lower zero-order rates.[102,103] Therefore, errors that result from the linearization can result in large differences in k_{max} and K_S estimates.

Michaelis-Menten kinetics, in general, describes the formation of a product by the activity of enzymes. Assuming PHE transformation by ELW1 can be described by Michaelis-Menten kinetics, and not additional processes were occurring, k_{max}/K_S should be constant and can be used to further evaluate the models. Normalizing the experimental first-order rate, k_{PHE}, by the biomass to obtain $k_{bio,PHE}$, is equivalent to k_{max}/K_S for each PHE mass tested (Table 2.3). The values for $k_{bio,PHE}$ ranged 0.0019-0.0059 L hr^{-1} mg^{-1} $protein^{-1}$ for PHE-exposed cells and 0.00012-0.0042 L hr^{-1} mg^{-1} $protein^{-1}$ for 1-octyne controls (Table 2.3). These values were generally not significantly similar for either type of reactor and suggested that cellular kinetics were different at different PHE masses for both PHE-exposed cells and 1-octyne controls.

Figure 2.5. Comparison of enzyme kinetic models, Model 1, Model 2, and Model 3 calculated from the Michaelis-Menten equation (eq. 2.1), to experimental results (n = 3). For Model 1, k_{max} and K_S were calculated by simultaneously solving both constants in the Michaelis-Menten equation based on a non-linear least squares method. For Model 2, K_S was the water solubility of PHE (6.7 µM) and k_{max} was calculated using the non-linear method. For Model 3, k_{max} and K_S were derived from a Lineweaver-Burk plot (Appendix A.12).

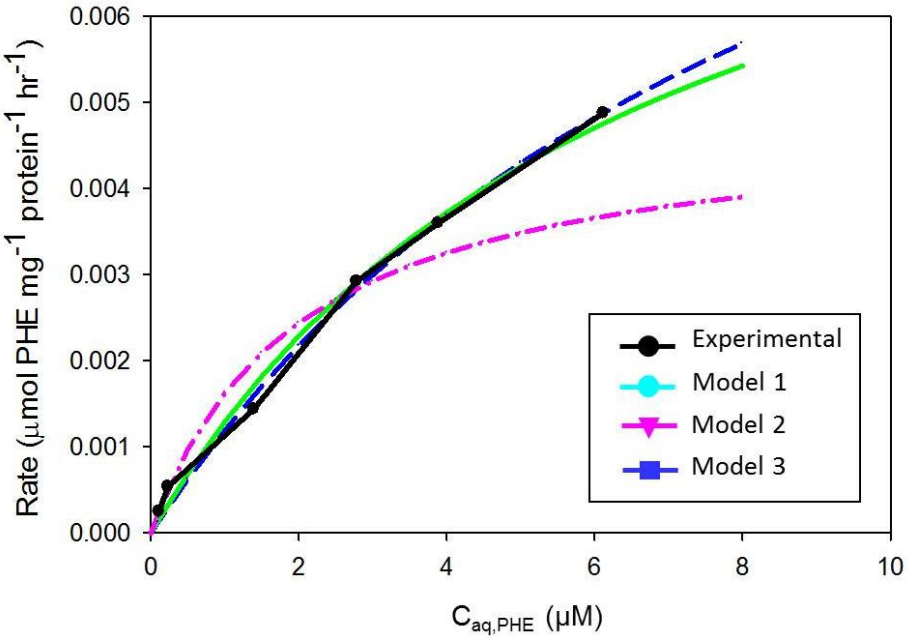

Table 2.4 Estimates for k_{max} and K_S used in three Michaelis-Menten models (eq 2.1). Model 1: non-linear method that simultaneously solved for k_{max} and K_S. Model 2: non-linear method with k_{max} equal to the water solubility of PHE (6.7 µM) and solving for K_S. Model 3: linearization method using Lineweaver-Burk plot (Appendix A.12).

Model Number	k_{max} (µmol mg^{-1} protein^{-1} hr^{-1})	K_S (µM)	k_{max}/K_S (L mg^{-1} protein^{-1} hr^{-1})
Model 1	0.0115	9.30	1.24×10^{-3}
Model 2	0.00999	6.73	1.48×10^{-3}
Model 3	0.00488	2.00	2.44×10^{-3}

Literature values of k_{max}, K_S, and k_{max}/K_S for several different microbes capable of degradation or cometabolism of single PAHs in aqueous systems are listed in Table 3.7. Literature values for k_{max}, K_S, and k_{max}/K_S were higher for PAHs that were degraded compared to those being co-metabolized. Experimental k_{max}/K_S, and modeled k_{max}, for this study were 2 - 3 magnitudes lower than values from other studies, and modeled K_S was generally 10 times higher than other studies. The deviation from reported kinetics indicates ELW1 does not have similar enzyme compared to *Sphingomonas* or *Novosphingobuim*. In addition, different models were used to estimate k_{max} and K_S in other studies, including Monod,[104] fourth order Rung-Kutta fitting method for Monod,[105] biomass partitioning and abiotic losses in Monod,[106] and dissolution of crystalized PAHs in Monod.[107] As far as the authors are aware, this is the first report of first-order cometabolism rates for PHE by a *Mycobacterium* sp.

Table 2.5. Literature values for k_{max} and K_S for several PAHs undergoing either degradation or cometabolism (comet) by different microbes. The ratio of k_{max} to K_S were either determined experimentally using biomass-normalized first-order transformation rates (Exp) or estimated by fitting a model to experimental data (Estimated). NAP: Napthalene, FLU: Fluorene, PHE: Phenanthrene, ANT: Anthracene.

PAH	Mechanism	k_{max} (µmol mg^{-1} $protein^{-1}$ hr^{-1})	K_S (µmol L^{-1})	k_{max}/K_S (L mg^{-1} $protein^{-1}$ hr^{-1})	Type of Data	Microbe	Ref
NAP	degradation	0.780	0.624	1.33	Estimated	*Sphingomonas paucimobilis* strain EPA509	105
NAP	degradation	4.962	4.463	1.11	Estimated	Mixed	104
FLU	comet	NA	NA	0.026	Exp	Mixed	104
FLU	degradation	0.241	0.120	2.6	Estimated	*Sphingomonas paucimobilis* strain EPA507	105
PHE	comet	NA	NA	0.27	Exp	Mixed	104
PHE	degradation	2.805	0.561	5	Estimated	*Novosphingobuim pentaromativorans* US6-1	107
PHE	degradation	2.805	0.561	5	Estimated	*Sphingomonas* sp EPA505	107
PHE	degradation	4.208	0.561	7.5	Estimated	*Sphingobuim yanoikuyae* B1	107
PHE	degradation	0.18	0.09	2.09	Estimated	*Sphingomonas paucimobilis* strain EPA505	106
PHE	comet	NA	NA	0.32	Exp	Mixed	104
PHE	comet	0.0048-0.012	2.0-9.30	0.0012-0.0024	Estimated	*Mycobacterium* sp. strain ELW1	This Study

2.4.3 Toxicity of PHE and OHPHE Metabolites

2.4.3.1. Embryonic Zebrafish Model

The developmental toxicity of PHE and OHPHE metabolite standards, were tested using the embryonic zebrafish model at concentrations ranging 0.1 – 50 µM. PHE and *trans*-9,10-PHE were not toxic to zebrafish. The other OHPHE metabolites were toxic with mean effective concentrations (EC_{50}) at 120 hours post fertilization

(hpf) decreasing (were more developmentally toxic) in the following order: 1-PHE >4-PHE > 3-PHE > 9-PHE > 1,9-PHE (Figure 2.6). Although EC_{50}s were determined at 120 hpf, the primary endpoint was mortality at 24 hpf.

Figure 2.6. Mean effective concentration (EC_{50}) at 120 hpf (with standard error bars, *n* = 32) of OHPHE standards in embryonic zebrafish. PHE and *trans*-9,10-PHE standards were not toxic to embryonic zebrafish.

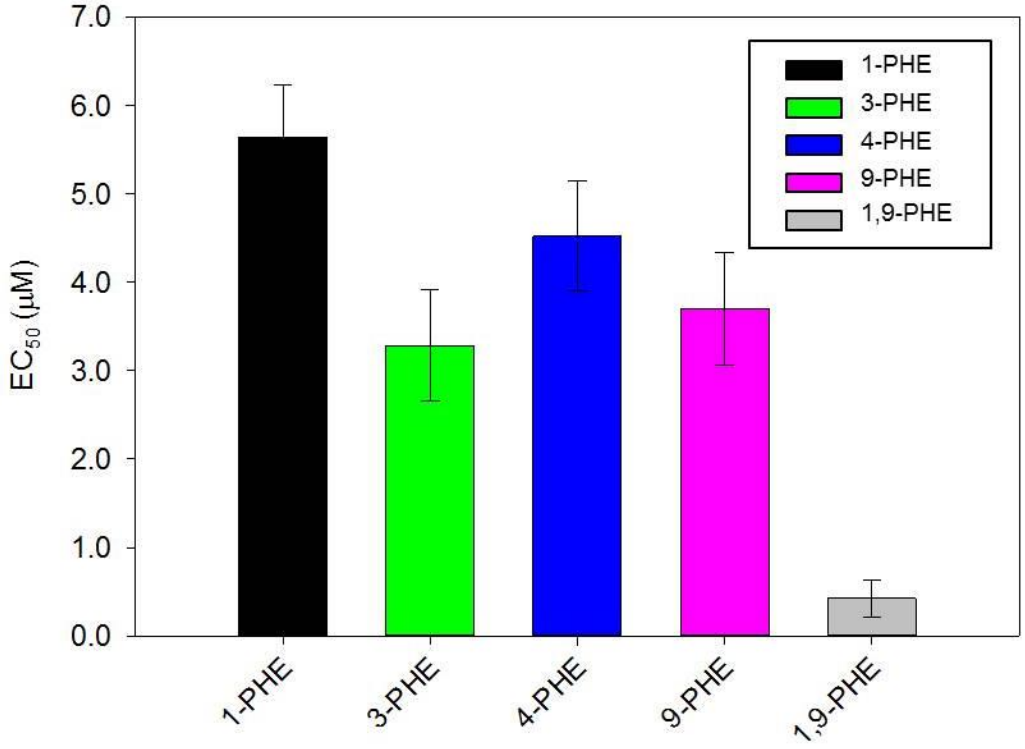

Metabolite mixtures formed by ELW1 in PHE-exposed cells, 1-octyne controls, and cell-only controls were also tested for developmental toxicity at concentrations ranging from 0.05 – 0.8 µM. Samples from each of the three aforementioned reactors were collected over five days (5, 28, 52, 76, and 122 hr) and each collection was tested using the embryonic zebrafish model. Toxicity was not observed for mixtures formed by ELW1 in 1-octyne controls and cells-only controls at any time. However, toxicity was observed for mixtures in PHE-exposed cells at 76

and 122 hrs, with EC_{50}s of 7.09 ± 1.12 (SE) and 9.60 ± 0.96 (SE) µM, respectively. The EC_{50}s for the mixture represents the total concentration of the all the toxic OHPHE metabolites, not individual OHPHEs, needed to elicit a toxic response.

As mentioned previously, embryonic zebrafish were exposed to five dilutions of metabolite mixtures. The concentrations of PHE and OHPHE metabolites in the mixtures at the lowest dilution (highest concentration) are shown in Figure 2.7. The yellow highlighted bars indicate the collection times that generated a toxic response. At the lowest dilution, the concentrations of the toxic metabolites tested on zebrafish were at least 1.5 times lower (Figure 2.7) than the concentrations needed to generate a toxic response based on the EC_{50}s for the standards (Figure 2.6).

To evaluate the contribution of the toxic mono-OHPHE metabolites (1-, 3-, 4-, and 9-PHE) and toxic di-OHPHE (1,9-PHE) compared to the non-toxic PHE and non-toxic *trans*-9,10-PHE over time, the ratio of both the sum of mono-OHPHE (Σ mono-OHPHE) (µM) and 1,9-PHE (µM) to the sum of non-toxic compounds (PHE and *trans*-9,10-PHE) was calculated over the time coarse of the experiment (Figure 2.8). There was not an obvious change in contribution of toxic OHPHE metabolites in PHE-exposed cells at 76 and 122 hr compared to the other time points or to 1-octyne controls (Figure 2.8). In additional, all QA/QC for the embryonic zebrafish testing were met.[95] Therefore, the toxicological response observed for PHE-exposed cells at 76 and 122 hr may have been a result of exposure to an unidentified PHE metabolite formed by ELW1.

Figure 2.7 Concentrations (n = 1) of PHE and OHPHE metabolites over time (hr) in the lowest dilution of the mixtures resulting from experiments with PHE-exposed cells (A) and 1-octyne-inhibited controls (B) tested on zebrafish. Note that the EC_{50} values for developmental toxicity (based on the embryonic zebrafish assays with the same mixtures) at 76 and 122 hr (highlighted in yellow) were 7.09 ± 1.12 (SE) and 9.60 ± 0.96 (SE) for the PHE-exposed cells. Significant differences are indicated by an asterisk (*).

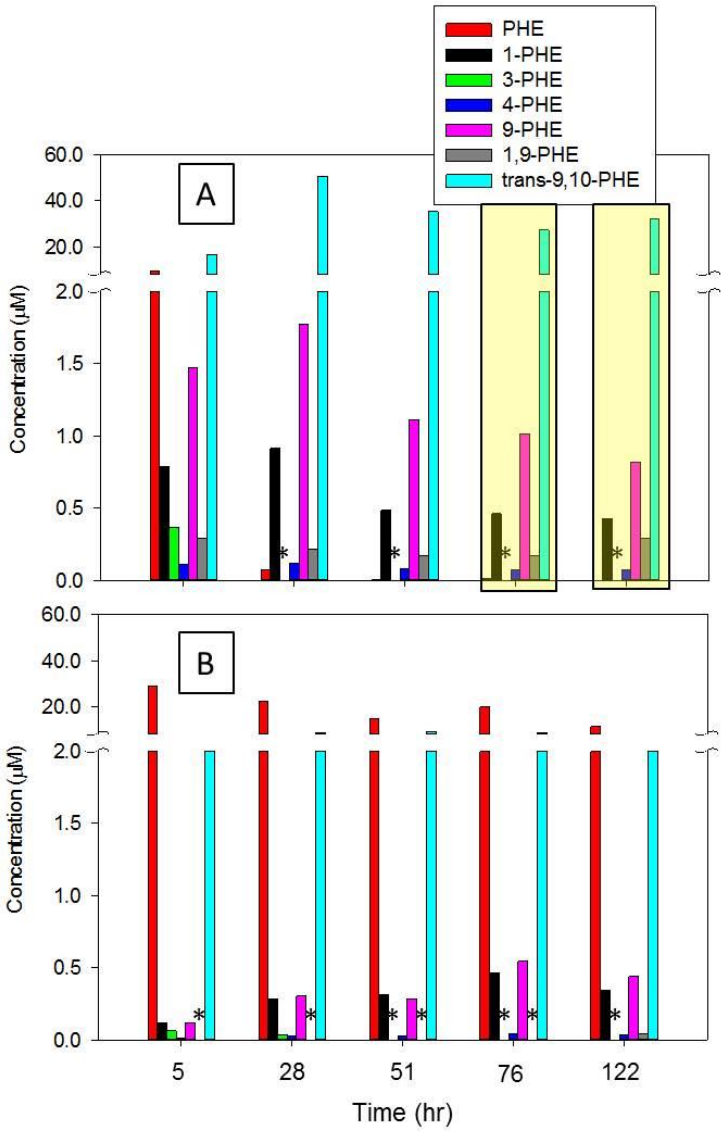

Figure 2.8. Ratios of the sum of toxic mono-OHPHEs (Σ Mono-OHPHE) and toxic 1,9-PHE, to the sum of non-toxic compounds (PHE and *trans*-9,10-PHE) over time in the PHE-exposed cells (A) and 1-octyne-inhibited controls (B) used in developmental toxicity testing with embryonic zebrafish. ND: Not detected.

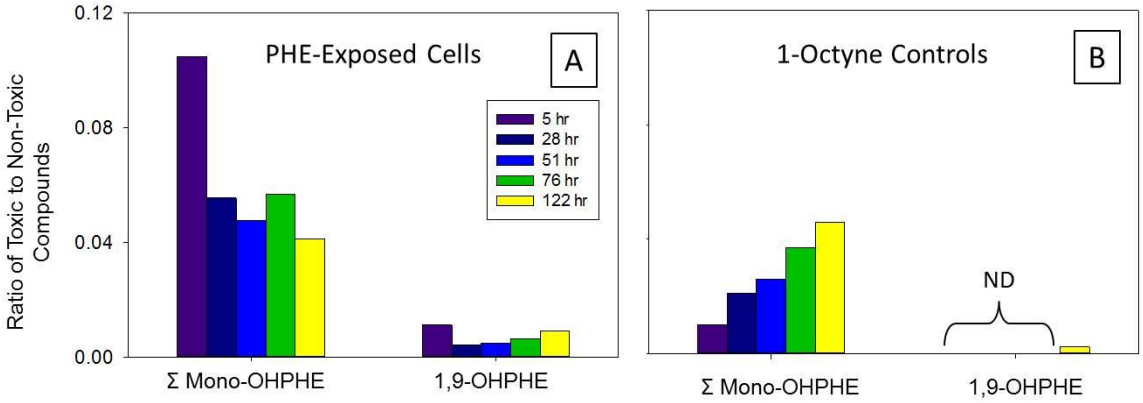

3.4.3.2. Cell Viability During PHE Exposure

The toxicity of OHPHE metabolites to ELW1 was evaluated by assessing cell viability of PHE-exposed cells, 1-octyne controls, and cell-only controls using live/dead cell staining and flow cytometry. The percent live cells (Appendix B.6) and the total number of cells (live + dead cells) (Figure 2.9) were measured over time. The percent live cells were consistently ~80% for all reactors over the course of the experiment (Appendix B.6). However, lower dilutions of cells were needed towards to the end of the experiment and this was not accounted for in the percent live cells results. Therefore, total number of cells (live + dead cells) was used. The total number of cells decreased for PHE-exposed cells, 1-octyne controls, and cells-only controls across the experimental period likely from cellular clumping of dead or compromised cells (Figure 2.9). However, the total number of cells exposed to 1.8 µmol PHE were statistically lower (p-value < 0.03) than the number of cells exposed

to 0.42 and 0.84 µmol at both 46 and 97 hr, 1-octyne controls, and cells-only controls (Figure 2.9). This indicates that cells exposed to 1.8 µmol PHE underwent more cell death, or were more severely compromised, than cells exposed to lower masses of PHE or the controls. The loss of cell viability over time may be a factor of PHE concentration, accumulation of OHPHE metabolites, and/or decreased activity from co-metabolism of resting cells.

Figure 2.9. Total number of cells (x1000) (with standard error bars, *n* = 3 except for 0.84 µmol PHE, *n* = 2) from live/dead cell staining for 1-octyne controls, cell-only controls, and PHE-exposed cells at 0.42, 0.84, and 1.8 µmol PHE. Significant differences are indicated by an asterisk (*).

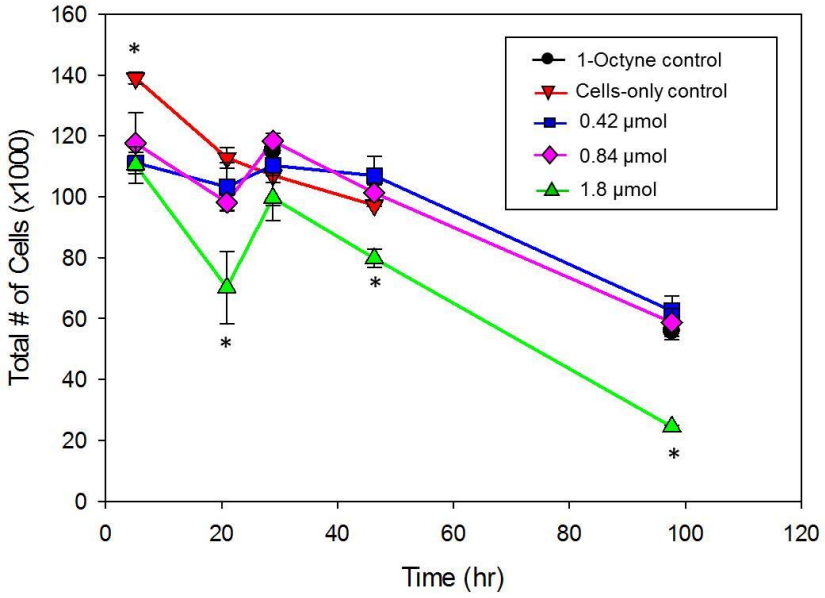

2.5 Conclusions

Mycobacterium sp. ELW1 was able to completely co-metabolize PHE within 48 hrs. Several OHPHE metabolites were formed, including a primary metabolite, *trans*-9,10-PHE, and minor products 1-PHE, 3-PHE, 4-PHE, 9-PHE, and 1-9-PHE. The primary metabolite made up 90% of the total metabolites formed. Zero-order rates for PHE transformation and metabolite formation were compared and showed good agreement. PHE transformation tended to follow first-order rates. Experimental

results were modeled using Michaelis-Menten kinetics after estimating k_{max} and K_S with non-linear and linearization methods. Non-linear estimates of k_{max} and K_S fit experimental results better. First order rates determined experimentally were normalized by biomass and represented the ratio of k_{max} to K_S and were 2-3 orders of magnitude lower than literature values determined for microbes other than *Mycobacterium* sp. using different models that incorporated additional parameters. OHPHE standards, including 1-PHE, 3-PHE, 4-PHE, 9-PHE, and 1,9-PHE, were developmentally toxic to zebrafish. However, PHE and *trans*-9,10-PHE were not. Mixtures of metabolites formed by ELW1 were not toxic but mixtures formed at 76 hr and 122 hr by PHE-exposed cells were toxic, possibly due to the formation of an unidentified toxic metabolite. In general, ELW1 formed toxic metabolites after exposure to PHE, but the concentrations were too low to elicit a toxic response in zebrafish.

2.6 Acknowledgements

This publication was made possible in part by grant number P30ES00210 from the National Institute of Environmental Health Sciences (NIEHS), National Institutes of Health (NIH), and NIEHS Grants P42 ES016465, P42 ES005948, and P30-ES10126. Its contents are solely the responsibility of the authors and do not necessarily represent the official view of the NIEHS, NIH. The authors would also like to thank Sinnhuber Aquatic Research Laboratory (SARL) for performing the toxicology testing, and Fan Wu and Stacey Harper for training and use of the flow cytometer for live/dead cells staining.

CHAPTER 3

CONCLUSIONS AND FUTURE DIRECTIONS

Mycobacterium sp. ELW1 was able to completely co-metabolize PHE, at different concentrations below its water solubility limit, in an aqueous system. The alkene monooxygenases in ELW1, used to initiate oxidation of PHE, were effectively inhibited by 1-octyne, however some PHE transformation was still observed possibly by enzymes not inhibited by 1-octyne. PHE metabolites measured consisted of only OHPHEs, with the primary product, *trans*-9,10-PHE, comprising more than 90% of the total metabolites formed in both PHE-exposed cells and 1-octyne controls. Other OHPHE that were measured were 1-PHE, 3-PHE, 4-PHE, 9-PHE, and 1-9-PHE.

Mass balances were estimated by summing the zero-order formation rates of OHPHE metabolites and comparing these to the zero-order transformation rates of PHE. The formation rates of OHPHE in PHE-exposed cells were in good agreement with the transformation rate of PHE. However, this method was not as useful for 1-octyne controls, since the sum of the OHPHE formation rates were either too high or too low compared to the transformation rate of PHE. The rate of abiotic losses, PHE adsorption to the glass reactor bottles, was not accounted in this estimate.

Michaelis-Menten kinetics was modeled using the zero-order rate of PHE transformation. Since PHE transformation experiments were limited by the water solubility of PHE, Michaelis-Menten variables, including the maximum rate, k_{max}, and the half-saturation constant, K_S, were not able to be determined experimentally.

These parameters were estimated using non-linear and linearization methods to generate three sets of k_{max} and K_S values. All three sets of k_{max} to K_S were then used to predict aqueous PHE concentrations with time. Estimates of k_{max} to K_S determined through non-linear methods more accurately fit experimental results than the values estimated using the linearization method.

Experimentally determined first-order PHE transformation rates that, when normalized by biomass, were equivalent to the ratio of the Michaelis-Menten kinetic variables k_{max} to K_S. Assuming the transformation of PHE by ELW1 followed Michaelis-Menten first-order kinetics, and also assuming no other processes were occurring, the ratio of k_{max} to K_S should be similar for all PHE concentrations. The ratio was not statistically similar for all PHE concentrations in both PHE-expose cells and 1-octyne control reactors. This suggests that there was a change in the cellular kinetics, including the cellular energy diminishing over time or the cells experienced a toxic effect by PHE and/or the metabolites, between the different experiments.

The zebrafish model was used to determine the developmental toxicity, if any, of OHPHE individual standards and the metabolite mixtures formed by ELW1 over time. OHPHE standards, including 1-PHE, 3-PHE, 4-PHE, 9-PHE, and 1,9-PHE, were developmentally toxic to zebrafish but not PHE or *trans*-9,10-PHE. Mixtures of metabolites, which sometimes also included PHE, formed by PHE-exposed cells, 1-octyne-controls, and cells-only controls over the course of 5 days, were not toxic to zebrafish, except for the mixture formed at 76 hr and 122 hr by PHE-exposed cells. The concentration of toxic metabolites tested on zebrafish was below the EC_{50}s determined from the OHPHE standards. Therefore, the concentrations were not high

enough to elicit a toxic response at all time point, including 76 hr and 122 hr. The ratio of the sum of toxic metabolites to the sum of non-toxic compounds (PHE and *trans*-9,10-PHE) at these later time points did not vary from the other time points in either PHE-exposed cells or 1-octyne controls. The toxic response at these times was possibly caused by the formation of an unidentified toxic metabolite.

The potential for ELW1 to be used for bioremediation still needs further investigation. Thus far, ELW1 has only been evaluated for the co-metabolism of PHE and there are many other microorganisms capable of degrading PHE and larger-ringed PAHs. ELW1 also transforms PHE at slower first-order rate than other microorganisms. However, the potential for ELW1 to co-metabolism larger-ringed PAHs is possible and efforts to investigate this capability should be made. OHPAH metabolites are more polar, and therefore more bioavailable, than the unsubstituted parent PAHs. Formation of polar metabolites through co-metabolism may be an important step in further transformation or degradation of larger-ringed PAHs.

Future directions for ELW1 and its capability to transform PAHs, and the potential toxicity of the metabolites, involve several additional experiments. First, the pathway for 1,9-PHE formation needs to be investigated. To do this, ELW1 will be exposed to 1-PHE and 9-PHE individually at concentrations close to the water solubility limit of PHE. The concentration of both 1-PHE and 9-PHE, as well as 1,9-PHE and additional metabolites, will be monitored over time using the method described in Chapter 2. Second, the possibility of *trans*-9,10-PHE transformation by ELW1 is of interest. This will be studied by exposing ELW1 to *trans*-9,10-PHE and monitoring concentration changes and product formation over time. Third, OHPHE

standard mixtures prepared in similar ratios to the mixtures produced by ELW1 will be further studied using the zebrafish model. Testing toxicity of standard mixtures will help clarify the cause behind toxic responses observed in mixtures produced by ELW1. The results from these experiments will be added to Chapter 2 prior to publication. Long-term future directions are to continue to study the capability of ELW1 to transform other PAHs, including four-ringed PAHs fluoranthene and pyrene, and known-carcinogen five-ringed PAH, benzo[a]pyrene. The toxicity of metabolites formed from these larger PAHs should to be tested.

Bibliography

(1) Registry, A. f. T. S. a. D., Public Health Statement: Polycyclic Aromatic Hydrocarbons (Pahs). In Services, D. o. H. a. H., Ed. www.atsdr.cdc.gov, 1995; pp 1-6.

(2) Kriech, A. J.; Kurek, J. T.; Osborn, L. V.; Wissel, H. L.; Sweeney, B. J., Determination of Polycyclic Aromatic Compounds in Asphalt and in Corresponding Leachate Water. *Polycyclic Aromatic Compounds* **2002**, *22*, (3-4), 517-535.

(3) Neff, J. M.; Stout, S. A.; Gunster, D. G., Ecological Risk Assessment of Polycyclic Aromatic Hydrocarbons in Sediments: Identifying Sources and Ecological Hazard. *Integrated Environmental Assessment and Management* **2005**, *1*, (1), 22-33.

(4) Fetzer, J. C.; Kershaw, J. R., Identification of Large Polycyclic Aromatic-Hydrocarbons in a Coal-Tar Pitch. *Fuel* **1995**, *74*, (10), 1533-1536.

(5) Ledesma, E. B.; Kalish, M. A.; Nelson, P. F.; Wornat, M. J.; Mackie, J. C., Formation and Fate of Pah During the Pyrolysis and Fuel-Rich Combustion of Coal Primary Tar. *Fuel* **2000**, *79*, (14), 1801-1814.

(6) Schubert, P.; Schantz, M. M.; Sander, L. C.; Wise, S. A., Determination of Polycyclic Aromatic Hydrocarbons with Molecular Weight 300 and 302 in Environmental-Matrix Standard Reference Materials by Gas Chromatography/Mass Spectrometry. *Analytical Chemistry* **2003**, *75*, (2), 234-246.

(7) Gevao, B.; Jones, K. C., Kinetics and Potential Significance of Polycyclic Aromatic Hydrocarbon Desorption from Creosote-Treated Wood. *Environmental Science & Technology* **1998**, *32*, (5), 640-646.

(8) Kohler, M.; Kunniger, T.; Schmid, P.; Gujer, E.; Crockett, R.; Wolfensberger, M., Inventory and Emission Factors of Creosote, Polycyclic Aromatic Hydrocarbons (Pah), and Phenols from Railroad Ties Treated with Creosote. *Environmental Science & Technology* **2000**, *34*, (22), 4766-4772.

(9) Cancer), I. I. A. f. R. o. *Iarc Monographs on the Evaluation of Carcinogenic Risks to Humans. In: Some Non-Heterocyclic Polycyclic Aromatic Hydrocarbons and Some Related Exposures.*; World Health Organization: Lyon, France, **2010**.

(10) Dean-Ross, D.; Moody, J.; Cerniglia, C. E., Utilization of Mixtures of Polycyclic Aromatic Hydrocarbons by Bacteria Isolated from Contaminated Sediment. *Fems Microbiology Ecology* **2002**, *41*, (1), 1-7.

(11) Mallick, S.; Chakraborty, J.; Dutta, T. K., Role of Oxygenases in Guiding Diverse Metabolic Pathways in the Bacterial Degradation of Low-Molecular-Weight Polycyclic Aromatic Hydrocarbons: A Review. *Critical Reviews in Microbiology* **2011**, *37*, (1), 64-90.

(12) Agency, U. S. E. P. Integrated Risk Information System (Iris). https://www.epa.gov/iris (July 10, 2016).

(13) Agency, U. S. E. P. Toxic and Priority Pollutants under the Clean Water Act. https://www.epa.gov/eg/toxic-and-priority-pollutants-under-clean-water-act (July 10, 2016).

(14) Wild, S. R.; Jones, K. C., Polynuclear Aromatic-Hydrocarbons in the United-Kingdom Environment - a Preliminary Source Inventory and Budget. *Environmental Pollution* **1995**, *88*, (1), 91-108.

(15) Gan, S.; Lau, E. V.; Ng, H. K., Remediation of Soils Contaminated with Polycyclic Aromatic Hydrocarbons (Pahs). *Journal of Hazardous Materials* **2009**, *172*, (2–3), 532-549.

(16) Bastida, F.; Jehmlich, N.; Lima, K.; Morris, B. E. L.; Richnow, H. H.; Hernandez, T.; von Bergen, M.; Garcia, C., The Ecological and Physiological Responses of the Microbial Community from a Semiarid Soil to Hydrocarbon Contamination and Its Bioremediation Using Compost Amendment. *Journal of Proteomics* **2016**, *135*, 162-169.

(17) Louati, H.; Ben Said, O.; Soltani, A.; Got, P.; Cravo-Laureau, C.; Duran, R.; Aissa, P.; Pringault, O.; Mahmoudi, E., Biostimulation as an Attractive Technique to Reduce Phenanthrene Toxicity for Meiofauna and Bacteria in Lagoon Sediment. *Environmental Science and Pollution Research* **2014**, *21*, (5), 3670-3679.

(18) Louati, H.; Ben Said, O.; Got, P.; Soltani, A.; Mahmoudi, E.; Cravo-Laureau, C.; Duran, R.; Aissa, P.; Pringault, O., Microbial Community Responses to Bioremediation Treatments for the Mitigation of Low-Dose Anthracene in Marine Coastal Sediments of Bizerte Lagoon (Tunisia). *Environmental Science and Pollution Research* **2013**, *20*, (1), 300-310.

(19) Adams, G. O.; Fufeyin, P. T.; Okoro, S. E.; Ehinomen, I., Bioremediation, Biostimulation and Bioaugmention: A Review. *International Journal of Environmental Bioremediation & Biodegradation* **2015**, *3*, (1), 28-39.

(20) Kastner, M.; Miltner, A., Application of Compost for Effective Bioremediation of Organic Contaminants and Pollutants in Soil. *Applied Microbiology and Biotechnology* **2016**, *100*, (8), 3433-3449.

(21) Margesin, R.; Schinner, F., Bioremediation (Natural Attenuation and Biostimulation) of Diesel-Oil-Contaminated Soil in an Alpine Glacier Skiing Area. *Applied and Environmental Microbiology* **2001**, *67*, (7), 3127-3133.

(22) Festa, S.; Coppotelli, B. M.; Morelli, I. S., Bacterial Diversity and Functional Interactions between Bacterial Strains from a Phenanthrene-Degrading Consortium Obtained from a Chronically Contaminated-Soil. *International Biodeterioration & Biodegradation* **2013**, *85*, 42-51.

(23) Festa, S.; Coppotelli, B. M.; Morelli, I. S., Comparative Bioaugmentation with a Consortium and a Single Strain in a Phenanthrene-Contaminated Soil: Impact on the Bacterial Community and Biodegradation. *Applied Soil Ecology* **2016**, *98*, 8-19.

(24) Wu, M.; Dick, W. A.; Li, W.; Wang, X.; Yang, Q.; Wang, T.; Xu, L.; Zhang, M.; Chen, L., Bioaugmentation and Biostimulation of Hydrocarbon Degradation and the Microbial Community in a Petroleum-Contaminated Soil. *International Biodeterioration & Biodegradation* **2016**, *107*, 158-164.

(25) Halsey, K. H.; Sayavedra-Soto, L. A.; Bottomley, P. J.; Arp, D. J., Trichloroethylene Degradation by Butane-Oxidizing Bacteria Causes a Spectrum of Toxic Effects. *Applied Microbiology and Biotechnology* **2005**, *68*, (6), 794-801.

(26) Nzila, A., Update on the Cometabolism of Organic Pollutants by Bacteria. *Environmental Pollution* **2013**, *178*, 474-482.

(27) Chauhan, A.; Fazlurrahman; Oakeshott, J. G.; Jain, R. K., Bacterial Metabolism of Polycyclic Aromatic Hydrocarbons: Strategies for Bioremediation. *Indian Journal of Microbiology* **2008**, *48*, (1), 95-113.

(28) Mackay, D.; Shiu, W. Y.; Ma, K.-C.; Lee, S. C., *Handbook of Physical-Chemical Properties and Environmental Fate for Organic Chemicals: Introduction and Hydrocarbons*. 2nd Edition ed.; Taylor & Francis Group: Boca Raton, FL, 2006; Vol. 1.

(29) Furukawa, K.; Suenaga, H.; Goto, M., Biphenyl Dioxygenases: Functional Versatilities and Directed Evolution. *J. Bacteriol.* **2004**, *186*, (16), 5189-5196.

(30) Ferraro, D. J.; Okerlund, A. L.; Mowers, J. C.; Ramaswamy, S., Structural Basis for Regioselectivity and Stereoselectivity of Product Formation by Naphthalene 1,2-Dioxygenase. *J. Bacteriol.* **2006**, *188*, (19), 6986-6994.

(31) Resnick, S. M.; Lee, K.; Gibson, D. T., Diverse Reactions Catalyzed by Naphthalene Dioxygenase from Pseudomonas Sp Strain Ncib 9816. *Journal of Industrial Microbiology & Biotechnology* **1996**, *17*, (5-6), 438-457.

(32) Selifonov, S. A.; Grifoll, M.; Eaton, R. W.; Chapman, P. J., Oxidation of Naphthenoaromatic and Methyl-Substituted Aromatic Compounds by Naphthalene 1,2-Dioxygenase. *Applied and Environmental Microbiology* **1996**, *62*, (2), 507-514.

(33) Schuler, L.; Jouanneau, Y.; Chadhain, S. M. N.; Meyer, C.; Pouli, M.; Zylstra, G. J.; Hols, P.; Agathos, S. N., Characterization of a Ring-Hydroxylating Dioxygenase from Phenanthrene-Degrading Sphingomonas Sp Strain Lh128 Able to Oxidize Benz a Anthracene. *Applied Microbiology and Biotechnology* **2009**, *83*, (3), 465-475.

(34) Jouanneau, Y.; Meyer, C.; Jakoncic, J.; Stojanoff, V.; Gaillard, J., Characterization of a Naphthalene Dioxygenase Endowed with an Exceptionally Broad Substrate Specificity toward Polycyclic Aromatic Hydrocarbons. *Biochemistry* **2006**, *45*, (40), 12380-12391.

(35) Vila, J.; Lopez, Z.; Sabate, J.; Minguillon, C.; Solanas, A. M.; Grifoll, M., Identification of a Novel Metabolite in the Degradation of Pyrene by Mycobacterium Sp Strain Ap1: Actions of the Isolate on Two- and Three-Ring Polycyclic Aromatic Hydrocarbons. *Applied and Environmental Microbiology* **2001**, *67*, (12), 5497-5505.

(36) Zhong, Y.; Zou, S. C.; Lin, L.; Luan, T. G.; Qiu, R. L.; Tam, N. F. Y., Effects of Pyrene and Fluoranthene on the Degradation Characteristics of Phenanthrene in the Cometabolism Process by Sphingomonas Sp. Strain Pheb4 Isolated from Mangrove Sediments. *Marine Pollution Bulletin* **2010**, *60*, (11), 2043-2049.

(37) Krivobok, S.; Kuony, S.; Meyer, C.; Louwagie, M.; Willison, J. C.; Jouanneau, Y., Identification of Pyrene-Induced Proteins in Mycobacterium Sp Strain 6py1: Evidence for Two Ring-Hydroxylating Dioxygenases. *J. Bacteriol.* **2003**, *185*, (13), 3828-3841.

(38) Kweon, O.; Kim, S. J.; Freeman, J. P.; Song, J.; Baek, S.; Cerniglia, C. E., Substrate Specificity and Structural Characteristics of the Novel Rieske Nonheme Iron Aromatic Ring-Hydroxylating Oxygenases Nidab and Nida3b3 from Mycobacterium Vanbaalenii Pyr-1. *Mbio* **2010**, *1*, (2).

(39) Seo, J.-S.; Keum, Y.-S.; Li, Q. X., Comparative Protein and Metabolite Profiling Revealed a Metabolic Network in Response to Multiple Environmental Contaminants in Mycobacterium Aromativorans Js19b1t. *Journal of Agricultural and Food Chemistry* **2011**, *59*, (7), 2876-2882.

(40) Baboshin, M. A.; Golovleva, L. A., Aerobic Bacterial Degradation of Polycyclic Aromatic Hydrocarbons (Pahs) and Its Kinetic Aspects. *Microbiology* **2012**, *81*, (6), 639-650.

(41) Kim, S. J.; Kweon, O.; Freeman, J. P.; Jones, R. C.; Adjei, M. D.; Jhoo, J. W.; Edmondson, R. D.; Cerniglia, C. E., Molecular Cloning and Expression of Genes Encoding a Novel Dioxygenase Involved in Low- and High-Molecular-Weight Polycyclic Aromatic Hydrocarbon Degradation in Mycobacterium Vanbaalenii Pyr-1. *Applied and Environmental Microbiology* **2006**, *72*, (2), 1045-1054.

(42) Van de Wiele, T.; Vanhaecke, L.; Boeckaert, C.; Peru, K.; Headley, J.; Verstraete, W.; Siciliano, S., Human Colon Microbiota Transform Polycyclic Aromatic Hydrocarbons to Estrogenic Metabolites. *Environmental Health Perspectives* **2005**, *113*, (1), 6-10.

(43) Jaiswal, P. K.; Gupta, J.; Shahni, S.; Thakur, I. S., Nadph Oxidase-Mediated Superoxide Production by Intermediary Bacterial Metabolites of Dibenzofuran: A Potential Cause for Trans-Mitochondrial Membrane Potential (Delta Im) Collapse in Human Hepatoma Cells. *Toxicol. Sci.* **2015**, *147*, (1), 17-27.

(44) Moorthy, B.; Chu, C.; Carlin, D. J., Polycyclic Aromatic Hydrocarbons: From Metabolism to Lung Cancer. *Toxicol. Sci.* **2015**, *145*, (1), 5-15.

(45) Chibwe, L.; Geier, M. C.; Nakamura, J.; Tanguay, R. L.; Aitken, M. D.; Simonich, S. L. M., Aerobic Bioremediation of Pah Contaminated Soil Results in Increased Genotoxicity and Developmental Toxicity. *Environmental Science & Technology* **2015**, *49*, (23), 13889-13898.

(46) Dubrovskaya, E. V.; Pozdnyakova, N. N.; Muratova, A. Y.; Turkovskaya, O. V., Changes in Phytotoxicity of Polycyclic Aromatic Hydrocarbons in the Course of Microbial Degradation. *Russian Journal of Plant Physiology* **2016**, *63*, (1), 172-179.

(47) Bücker, M.; Glatt, H. R.; Platt, K. L.; Avnir, D.; Ittah, Y.; Blum, J.; Oesch, F., Mutagenicity of Phenanthrene and Phenanthrene K-Region Derivatives. *Mutation Research* **1979**, *66*, (4), 337-348.

(48) Pagnout, C.; Rast, C.; Veber, A.-M.; Poupin, P.; Férard, J.-F., Ecotoxicological Assessment of Pahs and Their Dead-End Metabolites after Degradation by Mycobacterium Sp. Strain Snp11. *Ecotoxicology and Environmental Safety* **2006**, *65*, (2), 151-158.

(49) Kazunga, C.; Aitken, M. D.; Gold, A.; Sangaiah, R., Fluoranthene-2,3- and -1,5-Diones Are Novel Products from the Bacterial Transformation of Fluoranthene. *Environmental Science & Technology* **2001**, *35*, (5), 917-922.

(50) White, P. A., The Genotoxicity of Priority Polycyclic Aromatic Hydrocarbons in Complex Mixtures. *Mutation Research/Genetic Toxicology and Environmental Mutagenesis* **2002**, *515*, (1–2), 85-98.

(51) Martins, M.; Santos, J. M.; Diniz, M. S.; Ferreira, A. M.; Costa, M. H.; Costa, P. M., Effects of Carcinogenic Versus Non-Carcinogenic Ahr-Active Pahs and Their Mixtures: Lessons from Ecological Relevance. *Environmental Research* **2015**, *138*, 101-111.

(52) Michalec, F.-G.; Holzner, M.; Souissi, A.; Stancheva, S.; Barras, A.; Boukherroub, R.; Souissi, S., Lipid Nanocapsules for Behavioural Testing in Aquatic Toxicology: Time–Response of Eurytemora Affinis to Environmental Concentrations of Pahs and Pcb. *Aquatic Toxicology* **2016**, *170*, 310-322.

(53) Li, J.; Lu, S.; Liu, G.; Zhou, Y.; Lv, Y.; She, J.; Fan, R., Co-Exposure to Polycyclic Aromatic Hydrocarbons, Benzene and Toluene and Their Dose–Effects on Oxidative Stress Damage in Kindergarten-Aged Children in Guangzhou, China. *Science of The Total Environment* **2015**, *524–525*, 74-80.

(54) Søfteland, L.; Kirwan, J. A.; Hori, T. S. F.; Størseth, T. R.; Sommer, U.; Berntssen, M. H. G.; Viant, M. R.; Rise, M. L.; Waagbø, R.; Torstensen, B. E.; Booman, M.; Olsvik, P. A., Toxicological Effect of Single Contaminants and Contaminant Mixtures Associated with Plant Ingredients in Novel Salmon Feeds. *Food and Chemical Toxicology* **2014**, *73*, 157-174.

(55) Líbalová, H.; Krčková, S.; Uhlířová, K.; Milcová, A.; Schmuczerová, J.; Ciganek, M.; Kléma, J.; Machala, M.; Šrám, R. J.; Topinka, J., Genotoxicity but Not the Ahr-Mediated Activity of Pahs Is Inhibited by Other Components of Complex Mixtures of Ambient Air Pollutants. *Toxicology Letters* **2014**, *225*, (3), 350-357.

(56) Lewtas, J.; Walsh, D.; Williams, R.; Dobiáš, L., Air Pollution Exposure–DNA Adduct Dosimetry in Humans and Rodents: Evidence for Non-Linearity at High

Doses. *Mutation Research/Fundamental and Molecular Mechanisms of Mutagenesis* **1997**, *378*, (1–2), 51-63.

(57) Martins, M.; Santos, J. M.; Costa, M. H.; Costa, P. M., Applying Quantitative and Semi-Quantitative Histopathology to Address the Interaction between Sediment-Bound Polycyclic Aromatic Hydrocarbons in Fish Gills. *Ecotoxicology and Environmental Safety* **2016**, *131*, 164-171.

(58) Moody, J. D.; Freeman, J. P.; Doerge, D. R.; Cerniglia, C. E., Degradation of Phenanthrene and Anthracene by Cell Suspensions of Mycobacterium Sp Strain Pyr-1. *Applied and Environmental Microbiology* **2001**, *67*, (4), 1476-1483.

(59) Muratova, A.; Pozdnyakova, N.; Makarov, O.; Baboshin, M.; Baskunov, B.; Myasoedova, N.; Golovleva, L.; Turkovskaya, O., Degradation of Phenanthrene by the Rhizobacterium Ensifer Meliloti. *Biodegradation* **2014**, *25*, (6), 787-795.

(60) Moscoso, F.; Teijiz, I.; Deive, F. J.; Sanroman, M. A., Efficient Pahs Biodegradation by a Bacterial Consortium at Flask and Bioreactor Scale. *Bioresource Technology* **2012**, *119*, 270-276.

(61) Peng, L. B.; Deng, D. Y.; Ye, F. T., Efficient Oxidation of High Levels of Soil-Sorbed Phenanthrene by Microwave-Activated Persulfate: Implication for in Situ Subsurface Remediation Engineering. *J. Soils Sediments* **2016**, *16*, (1), 28-37.

(62) Mueller, J. G.; Lantz, S. E.; Blattmann, B. O.; Chapman, P. J., Bench-Scale Evaluation of Alternative Biological Treatment Processes for the Remediation of Pentachlorophenol- and Creosote-Contaminated Materials. Solid-Phase Bioremediation. *Environmental Science & Technology* **1991**, *25*, (6), 1045-1055.

(63) Bouchez, M.; Blanchet, D.; Bardin, V.; Haeseler, F.; Vandecasteele, J. P., Efficiency of Defined Strains and of Soil Consortia in the Biodegradation of Polycyclic Aromatic Hydrocarbon (Pah) Mixtures. *Biodegradation* **1999**, *10*, (6), 429-435.

(64) Richardson, S. D.; Aitken, M. D., Desorption and Bioavailability of Polycyclic Aromatic Hydrocarbons in Contaminated Soil Subjected to Long-Term in Situ Biostimulation. *Environmental Toxicology and Chemistry* **2011**, *30*, (12), 2674-2681.

(65) Hu, J.; Aitken, M. D., Desorption of Polycyclic Aromatic Hydrocarbons from Field-Contaminated Soil to a Two-Dimensional Hydrophobic Surface before and after Bioremediation. *Chemosphere* **2012**, *89*, (5), 542-547.

(66) Cébron, A.; Faure, P.; Lorgeoux, C.; Ouvrard, S.; Leyval, C., Experimental Increase in Availability of a Pah Complex Organic Contamination from an Aged Contaminated Soil: Consequences on Biodegradation. *Environmental Pollution* **2013**, *177*, (0), 98-105.

(67) Kappell, A. D.; Wei, Y.; Newton, R. J.; Van Nostrand, J. D.; Zhou, J. Z.; McLellan, S. L.; Hristova, K. R., The Polycyclic Aromatic Hydrocarbon Degradation Potential of Gulf of Mexico Native Coastal Microbial Communities after the Deepwater Horizon Oil Spill. *Frontiers in Microbiology* **2014**, *5*.

(68) Wilcke, W.; Kiesewetter, M.; Bandowe, B. A. M., Microbial Formation and Degradation of Oxygen-Containing Polycyclic Aromatic Hydrocarbons (Opahs) in Soil During Short-Term Incubation. *Environmental Pollution* **2014**, *184*, 385-390.

(69) Zhong, Y.; Luan, T.; Lin, L.; Liu, H.; Tam, N. F. Y., Production of Metabolites in the Biodegradation of Phenanthrene, Fluoranthene and Pyrene by the Mixed Culture of Mycobacterium Sp. And Sphingomonas Sp. *Bioresource Technology* **2011**, *102*, (3), 2965-2972.

(70) Isaac, P.; Martinez, F. L.; Bourguignon, N.; Sanchez, L. A.; Ferrero, M. A., Improved Pahs Removal Performance by a Defined Bacterial Consortium of Indigenous

Pseudomonas and Actinobacteria from Patagonia, Argentina. *International Biodeterioration & Biodegradation* **2015**, *101*, 23-31.

(71) Guo, M. X.; Gong, Z. Q.; Allinson, G.; Tai, P. D.; Miao, R. H.; Li, X. J.; Jia, C. Y.; Zhuang, J., Variations in the Bioavailability of Polycyclic Aromatic Hydrocarbons in Industrial and Agricultural Soils after Bioremediation. *Chemosphere* **2016**, *144*, 1513-1520.

(72) Boldrin, B.; Tiehm, A.; Fritzsche, C., Degradation of Phenanthrene, Fluorene, Fluoranthene, and Pyrene by a Mycobacterium Sp. *Applied and Environmental Microbiology* **1993**, *59*, (6), 1927-1930.

(73) Bouchez, M.; Blanchet, D.; Vandecasteele, J. P., The Microbiological Fate of Polycyclic Aromatic Hydrocarbons: Carbon and Oxygen Balances for Bacterial Degradation of Model Compounds. *Applied Microbiology and Biotechnology* **1996**, *45*, (4), 556-561.

(74) Tongpim, S.; Pickard, M. A., Cometabolic Oxidation of Phenanthrene to Phenanthrene Trans-9,10-Dihydrodiol by Mycobacterium Strain S1 Growing on Anthracene in the Presence of Phenanthrene. *Canadian Journal of Microbiology* **1999**, *45*, (5), 369-376.

(75) Pinyakong, O.; Habe, H.; Supaka, N.; Pinpanichkarn, P.; Juntongjin, K.; Yoshida, T.; Furihata, K.; Nojiri, H.; Yamane, H.; Omori, T., Identification of Novel Metabolites in the Degradation of Phenanthrene by Sphingomonas Sp. Strain P2. *FEMS Microbiology Letters* **2000**, *191*, (1), 115-121.

(76) van Herwijnen, R.; Wattiau, P.; Bastiaens, L.; Daal, L.; Jonker, L.; Springael, D.; Govers, H. A. J.; Parsons, J. R., Elucidation of the Metabolic Pathway of Fluorene and Cometabolic Pathways of Phenanthrene, Fluoranthene, Anthracene and Dibenzothiophene by Sphingomonas Sp. Lb126. *Research in Microbiology* **2003**, *154*, (3), 199-206.

(77) van Herwijnen, R.; van de Sande, B.; van der Wielen, F. W. M.; Springael, D.; Govers, H. A. J.; Parsons, J. R., Influence of Phenanthrene and Fluoranthene on the Degradation of Fluorene and Glucose by Sphingomonas Sp Strain Lb126 in Chemostat Cultures. *Fems Microbiology Ecology* **2003**, *46*, (1), 105-111.

(78) Leneva, N. A.; Kolomytseva, M. P.; Baskunov, B. P.; Golovleva, L. A., Phenanthrene and Anthracene Degradation by Microorganisms of the Genus Rhodococcus. *Applied Biochemistry and Microbiology* **2009**, *45*, (2), 169-175.

(79) Seo, J.-S.; Keum, Y.-S.; Hu, Y.; Lee, S.-E.; Li, Q. X., Phenanthrene Degradation in Arthrobacter Sp. P1-1: Initial 1,2-, 3,4- and 9,10-Dioxygenation, and Meta- and Ortho-Cleavages of Naphthalene-1,2-Diol after Its Formation from Naphthalene-1,2-Dicarboxylic Acid and Hydroxyl Naphthoic Acids. *Chemosphere* **2006**, *65*, (11), 2388-2394.

(80) Song, X. H.; Xu, Y.; Li, G. M.; Zhang, Y.; Huang, T. W.; Hu, Z., Isolation, Characterization of Rhodococcus Sp P14 Capable of Degrading High-Molecular-Weight Polycyclic Aromatic Hydrocarbons and Aliphatic Hydrocarbons. *Marine Pollution Bulletin* **2011**, *62*, (10), 2122-2128.

(81) Feng, T. C.; Cui, C. Z.; Dong, F.; Feng, Y. Y.; Liu, Y. D.; Yang, X. M., Phenanthrene Biodegradation by Halophilic Martelella Sp Ad-3. *Journal of Applied Microbiology* **2012**, *113*, (4), 779-789.

(82) Seo, J.-S.; Keum, Y.-S.; Li, Q. X., Mycobacterium Aromativorans Js19b1t Degrades Phenanthrene through C-1,2, C-3,4 and C-9,10 Dioxygenation Pathways. *International Biodeterioration & Biodegradation* **2012**, *70*, 96-103.

(83) Cerniglia, C. E., Biodegradation of Polycyclic Aromatic Hydrocarbons. *Current Opinion in Biotechnology* **1993**, *4*, (3), 331-338.

(84) Lu, X.-Y.; Zhang, T.; Fang, H. H.-P., Bacteria-Mediated Pah Degradation in Soil and Sediment. *Applied Microbiology and Biotechnology* **2011**, *89*, (5), 1357-1371.

(85) Yuan, J.; Lai, Q. L.; Sun, F. Q.; Zheng, T. L.; Shao, Z. Z., The Diversity of Pah-Degrading Bacteria in a Deep-Sea Water Column above the Southwest Indian Ridge. *Frontiers in Microbiology* **2015**, *6*.

(86) Pagnout, C.; Frache, G.; Poupin, P.; Maunit, B.; Muller, J. F.; Ferard, J. F., Isolation and Characterization of a Gene Cluster Involved in Pah Degradation in Mycobacterium Sp Strain Snp11: Expression in Mycobacterium Smegmatis Mc(2)155. *Research in Microbiology* **2007**, *158*, (2), 175-186.

(87) Kottegoda, S.; Wallgoram, E.; Hyman, M., Metabolism of 2-Methylpropene (Isobutylene) by the Aerobic Bacterium *Mycobacterium* Sp. Strain Elw1. *Journal of Applied and Environmental Microbiology* **2015**, *81*, (6), 1966-1976.

(88) House, A. J.; Hyman, M. R., Effects of Gasoline Components on Mtbe and Tba Cometabolism by Mycobacterium Austroafricanum Job5. *Biodegradation* **2010**, *21*, (4), 525-541.

(89) Kanaly, R. A.; Harayama, S., Biodegradation of High-Molecular-Weight Polycyclic Aromatic Hydrocarbons by Bacteria. *J. Bacteriol.* **2000**, *182*, (8), 2059-2067.

(90) Taylor, A. E.; Vajrala, N.; Giguere, A. T.; Gitelman, A. I.; Arp, D. J.; Myrold, D. D.; Sayavedra-Soto, L.; Bottomley, P. J., Use of Aliphatic *N*-Alkynes to Discriminate Soil Nitrification Activities of Ammonia-Oxidizing Thaumarchaea and Bacteria. *Journal of Applied and Environmental Microbiology* **2013**, *79*, (21), 6544-6551.

(91) Motorykin, O.; Schrlau, J.; Jia, Y.; Harper, B.; Harris, S.; Harding, A.; Stone, D.; Kile, M.; Sudakin, D.; Massey Simonich, S. L., Determination of Parent and Hydroxy Pahs in Personal Pm2.5 and Urine Samples Collected During Native American Fish Smoking Activities. *Science of The Total Environment* **2015**, *505*, 694-703.

(92) Schummer, C.; Delhomme, O.; Appenzeller, B. M. R.; Wennig, R.; Millet, M., Comparison of Mtbstfa and Bstfa in Derivatization Reactions of Polar Compounds Prior to Gc/Ms Analysis. *Talanta* **2009**, *77*, (4), 1473-1482.

(93) EPA Method - 8280a, Epa. The Analysis of of Polychlorinated Dibenzo-P-Dioxins and Polychlorinated Dibenzofurans by High-Resolution Gas Chromatography/Low Resolution Mass Spectrometry (Hrgc/Lrms).

(94) Johnson, K. A.; Goody, R. S., The Original Michaelis Constant: Translation of the 1913 Michaelis–Menten Paper. *Biochemistry* **2011**, *50*, (39), 8264-8269.

(95) Truong, L.; Bugel, S. M.; Chlebowski, A.; Usenko, C. Y.; Simonich, M. T.; Simonich, S. L. M.; Tanguay, R. L., Optimizing Multi-Dimensional High Throughput Screening Using Zebrafish. *Reproductive Toxicology* **2016**, *65*, 139-147.

(96) Truong, L.; Harper, S. L.; Tanguay, R. L., Evaluation of Embryotoxicity Using the Zebralfish Model. *Methods in Molecular Biology* **2011**, *691*, 271-279.

(97) Pinyakong, O.; Habe, H.; Kouzuma, A.; Nojiri, H.; Yamane, H.; Omori, T., Isolation and Characterization of Genes Encoding Polycyclic Aromatic Hydrocarbon Dioxygenase from Acenaphthene and Acenaphthylene Degrading Sphingomonas Sp. Strain A4. *FEMS Microbiology Letters* **2004**, *238*, (2), 297-305.

(98) Hennessee, C. T.; Li, Q. X., Effects of Polycyclic Aromatic Hydrocarbon Mixtures on Degradation, Gene Expression, and Metabolite Production in Four Mycobacterium Species. *Applied and Environmental Microbiology* **2016**, *82*, (11), 3357-3369.

(99) Hyman, M., Enzyme for the Pah Epoxide. In Genetic determinations for ELW1 ed.; Semprini, L., Ed. email, 2016.

(100) Wammer, K. H.; Peters, C. A., Polycyclic Aromatic Hydrocarbon Biodegradation Rates: A Structure-Based Study. *Environmental Science & Technology* **2005**, *39*, (8), 2571-2578.

(101) Sepic, E.; Bricelj, M.; Leskovsek, H., Biodegradation Studies of Polyaromatic Hydrocarbons in Aqueous Media. *Journal of Applied Microbiology* **1997**, *83*, (5), 561-568.

(102) Dowd, J. E.; Riggs, D. S., A Comparison of Estimates of Michaelis- Menten Kinetic Constants from Various Linear Transformations. *Journal of Biological Chemistry* **1965**, *240*, 863-869.

(103) Smith, K. E. C.; Rein, A.; Trapp, S.; Mayer, P.; Karlson, U. G., Dynamic Passive Dosing for Studying the Biotransformation of Hydrophobic Organic Chemicals: Microbial Degradation as an Example. *Environmental Science & Technology* **2012**, *46*, (9), 4852-4860.

(104) Knightes, C. D.; Peters, C. A., Aqueous Phase Biodegradation Kinetics of 10 Pah Compounds. *Environ. Eng. Sci.* **2003**, *20*, (3), 207-218.

(105) Desai, A. M.; Autenrieth, R. L.; Dimitriou-Christidis, P.; McDonald, T. J., Biodegradation Kinetics of Select Polycyclic Aromatic Hydrocarbon (Pah) Mixtures by Sphingomonas Paucimobilis Epa505. *Biodegradation* **2008**, *19*, (2), 223-233.

(106) Dimitriou-Christidis, P.; Autenrieth, R. L.; McDonald, T. J.; Desai, A. M., Measurement of Biodegradability Parameters for Single Unsubstituted and Methylated Polycyclic Aromatic Hydrocarbons in Liquid Bacterial Suspensions. *Biotechnology and Bioengineering* **2007**, *97*, (4), 922-932.

(107) Adam, I. K. U.; Rein, A.; Miltner, A.; Fulgêncio, A. C. D.; Trapp, S.; Kästner, M., Experimental Results and Integrated Modeling of Bacterial Growth on an Insoluble Hydrophobic Substrate (Phenanthrene). *Environmental Science & Technology* **2014**, *48*, (15), 8717-8726.

Appendices

Appendix A

Supporting Information for Chapter 2

Transformation of Phenanthrene by Mycobacterium sp. ELW1

and the Formation of Toxic Metabolites

Contents

Appendix A.1 Physical chemical properties for the US EPA 16 priority PAHs [1].

PAH	CAS	Rings	Formula	MW	Density (g/cm^3 at 20^oC)	Vapor Pressure (Pa at 25^oC)	Water Solubility (g/m^3 at 25^oC)	Henry's Law Constant (Pa m^3/mol)[a]	Log Kow	log Koc	Log Koa[b]
Naphthalene	91-20-3	2	C10H8	128.18	1.0	1.1E+01	3.0E+01	4.5E+01	3.4	3.0	5.1
Anthracene	120-12-7	3	C14H10	178.24	1.3	1.4E-03	7.5E-02	5.0E+00	4.5	4.4	7.1
Phenanthrene	85-01-8	3	C14H10	178.24	1.2	1.6E-02	1.2E+00	4.4E+00	4.5	4.3	7.2
Fluorene	86-73-7	3	C13H10	166.23	1.2	8.0E-02	1.9E+00	9.1E+00	4.2	4.2	6.6
Acenaphthene	83-32-9	3	C12H10	154.2	1.0	2.9E-01	4.0E+00	1.4E+01	3.7	3.6	6.0
Acenaphthylene	208-96-8	3	C12H8	152.2	0.90	8.9E-01	3.9E+00	1.2E+01	3.9	3.6	6.3
Chrysene	218-01-9	4	C18H12	228.3	1.3	4.0E-06	2.0E-03	4.4E-01	5.6	3.7	9.5
Benzo[a]-anthracene	56-55-3	4	C18H12	228.3	1.3	3.4E-05	1.0E-02	7.1E-01	5.9	5.3	9.1
Pyrene	129-00-0	4	C16H10	202.26	1.3	6.0E-04	1.3E-01	1.3E+00	5.0	4.8	8.2
Fluoranthene	206-44-0	4	C16H10	202.26	1.3	1.2E-03	2.4E-01	1.5E+00	5.2	4.6	8.6
Dibenz[a,h]-anthracene	53-70-3	5	C22H14	278.36	not listed	1.3E-08	5.0E-04	5.6E-03	6.4	6.5	11.8
Benzo[a]pyrene	50-32-8	5	C20H12	252.32	not listed	7.0E-07	3.0E-03	5.0E-02	6.0	6.7	10.9
Benzo[k]fluoranthene	207-08-9	5	C20H12	252.32	not listed	7.5E-07	7.0E-04	5.9E-02	6.4	5.7	10.7
Benzo[b]fluoranthene	205-99-22	5	C20H12	252.32	not listed	6.7E-05	1.4E-02	6.6E-02	6.5	5.7	10.4
Benzo[ghi]perylene	191-24-2	6	C22H12	276.34	not listed	1.4E-08	2.9E-04	3.3E-02	7.1	6.3	11.5
Indeno[1,2,3-cd]pyrene	193-39-5	6	C22H12	276.33	not listed	1.3E-07	1.9E-04	3.4E-02	7.7	8.0	11.6

[a]Ref [2], [b]EPI Suite 4.1

Appendix A.2 % Recovery of PHE and OHPHE over the analytical method (with standard error, $n = 3$)

Compound	Average % Recovery	SE
Phenanthrene	54.0	2.74
1-Hydroxynaphthalene	51.43	4.73
2-Hydroxynaphthalene	83.28	8.66
1,5-Dihydroxynaphthalene	23.56	15.00
1,6-Dihydroxynaphthalene	40.29	12.23
2,3-Dihydroxynaphthalene	24.44	15.90
2,6-Dihydroxynaphthalene	58.94	5.86
2,7-Dihydroxynaphthalene	92.41	7.40
1-OH-2-Naphthoic Acid	43.30	1.89
1-Hydroxyphenanthrene	70.94	1.47
2-Hydroxyphenanthrene	82.60	3.76
3-Hydroxyphenanthrene	81.77	3.96
4-Hydroxyphenanthrene	69.04	1.85
9-Hydroxyphenanthrene	44.68	8.83
1,9-Dihydroxyphenanthrene	18.76	6.12
cis-9,10-dihydroxy-9,10-dihydrophenanthrene	61.53	3.57
trans-9,10-dihydroxy-9,10-dihydrophenanthrene	51.43	4.73

Appendix A.3 Estimated Detection Limits (EDLs) for PHE and OHPHEs. PHE was quantified from phenanthrene-d10 and OHPAHs were quantified from the internal standard.

Analyte	Abbreviation	Surrogate	Internal Standard	EDL (pg μL^{-1})
Phenanthrene	PHE	Phenanthrene-d10	d_{10}-Acenaphthene	0.51
1-Hydroxynaphthalene	1-NAP	d_8-1-Hydroxynaphthalene	d_{10}-Acenaphthene	1.29
2-Hydroxynaphthalene	2- NAP	d_8-1-Hydroxynaphthalene	d_{10}-Acenaphthene	0.32
1,5-Dihydroxynaphthalene	1,5- NAP	d_8-1-Hydroxynaphthalene	d_{10}-Acenaphthene	0.41
1,6-Dihydroxynaphthalene	1,6- NAP	d_8-1-Hydroxynaphthalene	d_{10}-Acenaphthene	3.28
2,3-Dihydroxynaphthalene	2,3- NAP	d_8-1-Hydroxynaphthalene	d_{10}-Acenaphthene	0.74
2,6-Dihydroxynaphthalene	2,6- NAP	d_8-1-Hydroxynaphthalene	d_{10}-Acenaphthene	0.40
2,7-Dihydroxynaphthalene	2,7- NAP	d_8-1-Hydroxynaphthalene	d_{10}-Acenaphthene	0.73
1-Hydroxy-2-naphthoic acid	1-OH-2-NAP	d_8-1-Hydroxynaphthalene	d_{10}-Acenaphthene	0.43
1-Hydroxyphenanthrene	1-PHE	4-Hydroxy[$^{13}C_6$]phenanthrene	d_{10}-Acenaphthene	4.89
2-Hydroxyphenanthrene	2-PHE	4-Hydroxy[$^{13}C_6$]phenanthrene	d_{10}-Acenaphthene	3.15
3-Hydroxyphenanthrene	3-PHE	4-Hydroxy[$^{13}C_6$]phenanthrene	d_{10}-Acenaphthene	2.96
4-Hydroxyphenanthrene	4-PHE	4-Hydroxy[$^{13}C_6$]phenanthrene	d_{10}-Acenaphthene	0.86
9-Hydroxyphenanthrene	9-PHE	4-Hydroxy[$^{13}C_6$]phenanthrene	d_{10}-Acenaphthene	1.66
1,9-Dihydroxyphenanthrene	1,9-PHE	4-Hydroxy[$^{13}C_6$]phenanthrene	d_{10}-Acenaphthene	0.94
trans-9,10-dihydroxy-9,10-dihydrophenanthrene	*trans*-9,10-PHE	4-Hydroxy[$^{13}C_6$]phenanthrene	d_{10}-Acenaphthene	4.39
cis-9,10-dihydroxy-9,10-dihydrophenanthrene	*cis*-9,10-PHE	4-Hydroxy[$^{13}C_6$]phenanthrene	d_{10}-Acenaphthene	5.01

Appendix A.4 GC/MS EI SIM method parameters for the analysis of OHPAHs derivatized with BSTFA. MW-BSTFA is the MW of OHPAHs before derivatization and MW+BSTFA is the MW of OHPAHs after derivatization (MW-BSTFA + m/z 72). Ion fragments (m/z) refer to those formed from the MW+BSTFA OHPAHs where m/z 1: MW+BSTFA – 15 g mol^{-1}; m/z 2: MW+BSTFA – 89 g mol^{-1}; and m/z: MW+BSTFA – 31 g mol^{-1}. Acenaphthalene-d10 did not undergo derivatization. Therefore, fragments are those formed from MW-BSTFA. The quantification ion was m/z 1 and the qualification ions were m/z 2 and m/z 3.

Window	**Analyte**	**MW-BSTFA (g/mol)**	**MW+ BSTFA (g/mol)**	**m/z 1**	**m/z 2**	**m/z 3**	**Retention Time(min)**
1	d_{10}-Acenaphthalene	164	NA	162	164		8.903
	d_8-1-Hydroxynaphthalene	151	223	208	134	192	9.303
	1-Hydroxynaphthalene	144	216	201	127	185	9.328
	2-Hydroxynaphthalene	144	216	201	127	185	9.527
2	9-Hydroxyfluorene	182	254	239	165	223	11.875
	1,5-Dihydroxynaphthalene	160	304	289	215	273	12.59
	1,6-Dihydroxynaphthalene	160	304	289	215	273	12.932
	2,7-Dihydroxynaphthalene	160	304	289	215	273	13.306
	2,6-Dihydroxynaphthalene	160	304	289	215	273	13.464
	2,3-Dihydroxynaphthalene	160	304	289	215	273	13.659
3	3-Hydroxy[$^{13}C_6$]fluorene-	188	260	245	171	229	14.238
	3-Hydroxyfluorene	182	254	239	165	223	14.239
	2-Hydroxyfluorene	182	254	239	165	223	14.655
	1-OH-2-Naphthoic acid		332	317	243	301	14.838
4	*trans*-9,10-Dihydroxy-9,10 dihydrophenanthrene	212	356	341	267	325	15.695
	1-Hydroxy-9-fluorenone	196	268	253	179	237	15.97
	4-Hydroxy[$^{13}C_4$] phenanthrene	198	270	255	181	239	16.286
	4-Hydroxyphenanthrene	194	266	251	177	235	16.286
5	9-Hydroxyphenanthrene	194	266	251	177	235	16.944
	2-Hydroxy-9-fluorenone	196	268	253	179	237	17.16
	3-Hydroxyphenanthrene	194	266	251	177	235	17.401
	1-Hydroxyphenanthrene	194	266	251	177	235	17.476
	2-Hydroxyphenanthrene	194	266	251	177	235	17.943
	1,9-Dihydroxyphenanthrene	210	354	339	265	323	20.548

Appendix A.5 Structures of commercially-available OHPAHs

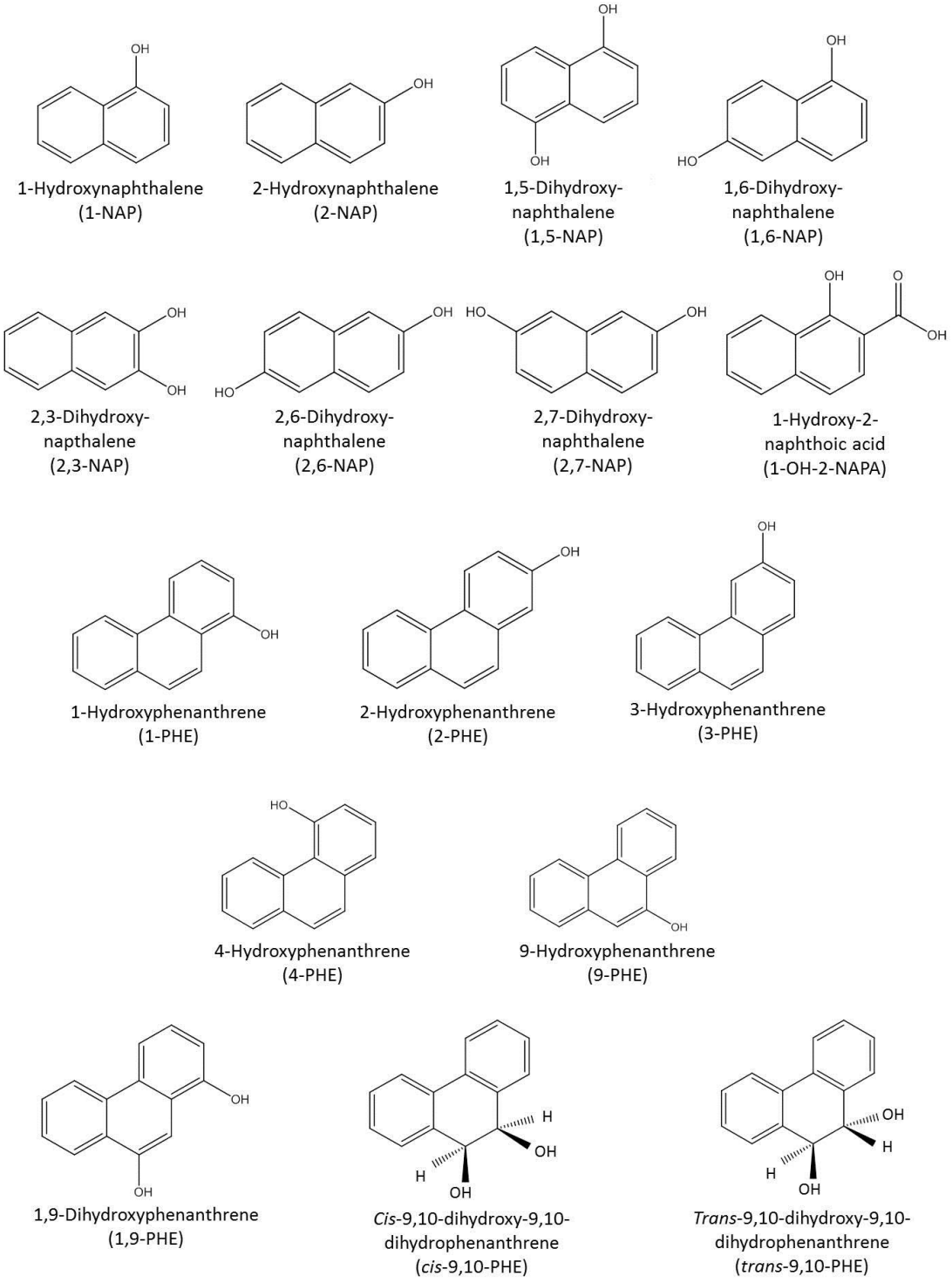

Appendix A.6. Biomass-normalized isobutene consumption by ELW1 without MeOH (Neg Control) and with 0.0089% MeOH (v/v) (with standard error bars, $n = 3$). Isobutene consumption was normalized by biomass (mg protein). Zero-order isobutene consumption rates, determined during the first hour (listed on the plot), were not statistically different ($p > 0.2$) indicating that 0.0089% MeOH (v/v) did not negatively affect the activity of ELW1.

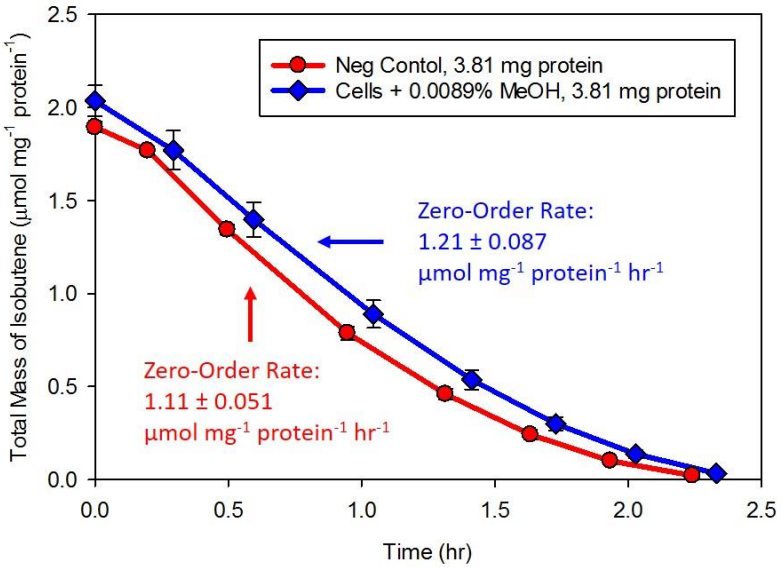

Appendix A.7. Biomass-normalized isobutene consumption by ELW1 in the presence of different aqueous concentrations of 1-octyne (with standard error bars, n = 3). Negative control, ●— ; 2.0 µmol L^{-1}, ◆— ; 5.3 µmol L^{-1}, ▼— ; 7.6 µmol L^{-1}, ○— ; 10 µmol L^{-1}, ■— ; 11 µmol L^{-1}, ▲— .

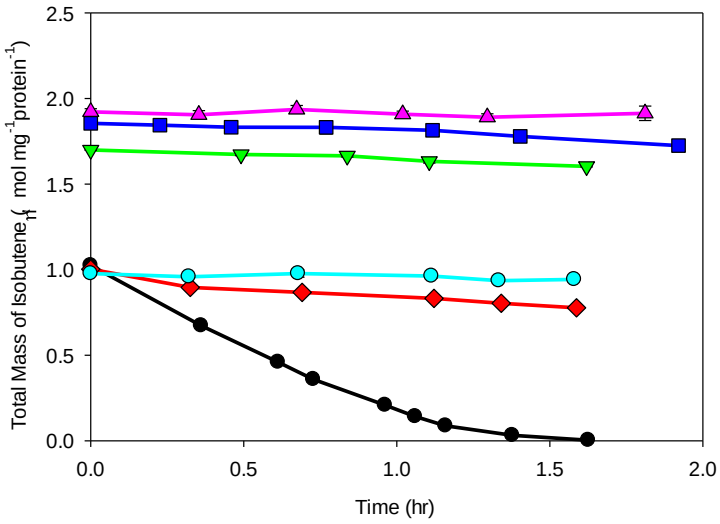

Appendix A.8. Biomass-normalized isobutene consumption rates (with standard error, n = 3) in the presence of different concentrations of gas-phase 1-octyne, determined during the first hour, from Appendix A.7. Consumption rates that were not statistically difference are designated by the same superscript letter.

1-Octyne C_{aq} (µM)	**Rate ± SE (µmol isobutene mg^{-1} protein^{-1} d^{-1})**
Negative Control	21.6 ± 0.156 ^{A}
2.0	3.97 ± 0.041 ^{B}
5.3	1.32 ± 0.121 ^{C}
7.6	2.05 ± 0.062 ^{C}
10	1.06 ± 0.013 ^{C}
11	0.485 ± 0.060 ^{D}

Appendix A.9. Biomass-normalized isobutene consumption by ELW1 in the absence of PHE (with standard error bars, *n* = 3). The lines represent the different batches of cells used in the different PHE exposure experiments indicated in the legend.

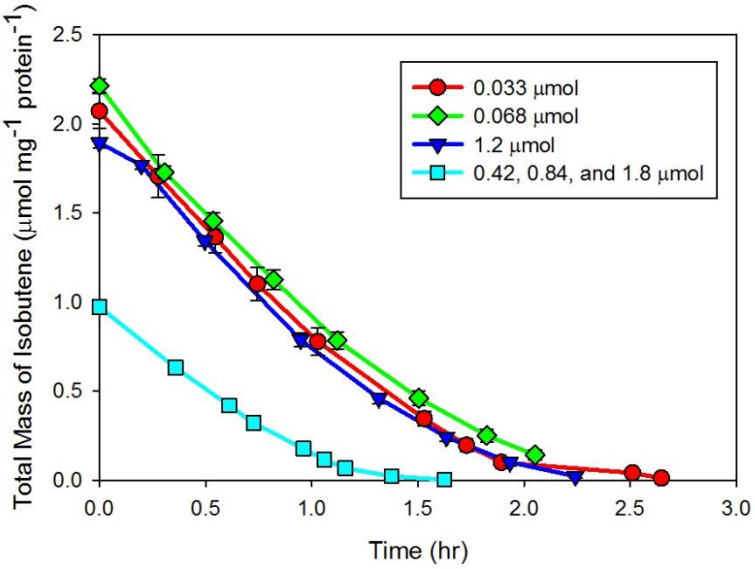

Appendix A.10. Biomass-normalized isobutene consumption rates (with standard errors, *n* = 3), determined during the first hour, from Appendix A.9. Consumption rates that were not statistically difference are designated by the same superscript letter.

Pre-Exposed Cells were Later used for PHE Mass (µmol)	Mass of ELW 1 (mg protein)	Isobutene Consumption Rate ± SE (µmol mg^{-1} $protein^{-1}$ hr^{-1})
0.033	3.84	1.26 ± 0.031^{A}
0.068	3.93	1.26 ± 0.017^{A}
1.2	3.81	1.21 ± 0.087^{A}
0.42, 0.84, and 1.8	5.05	0.899 ± 0.037^{B}

Appendix A.11. Natural log (ln) PHE transformation of six PHE masses (with standard error bars, n = 3 except for 1-octyne control exposed to 0.84 µmol PHE, n = 2) by ELW1 for PHE-exposed cells (solid lines) (A), 1-octyne controls (dashed lines) (B), and PHE-only control (dotted lines) (C).

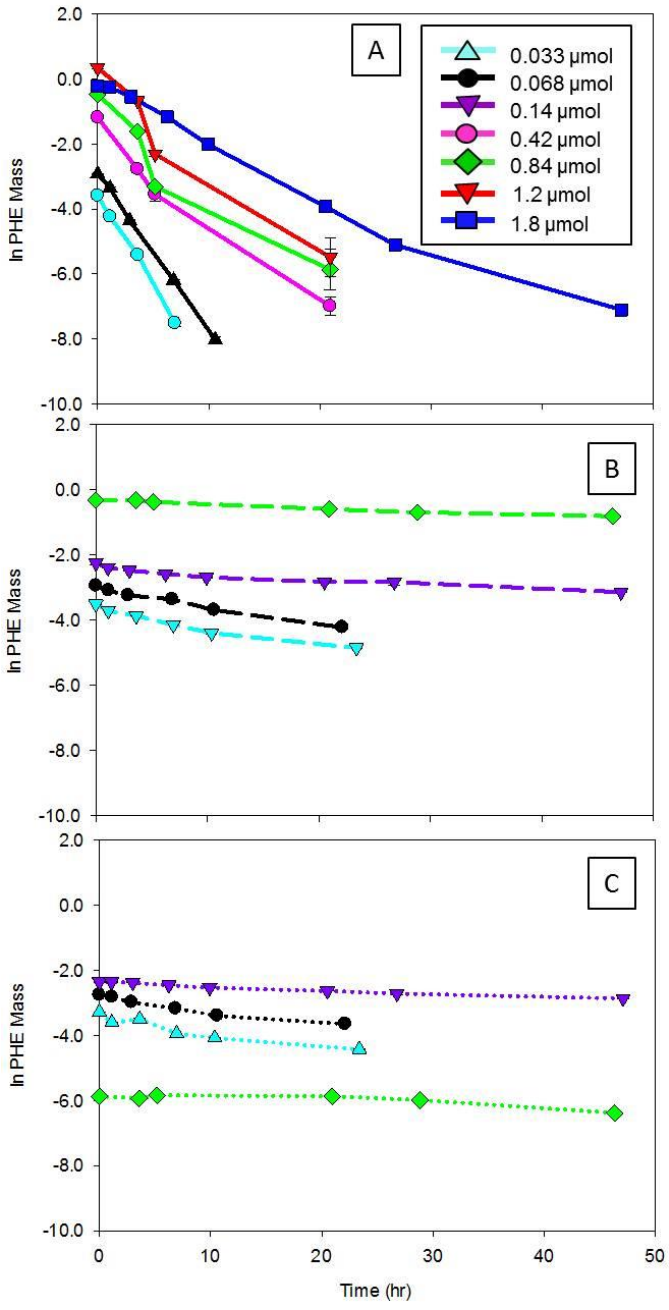

Appendix A.12. Lineweaver-Burk plot of biomass-normalized zero-order PHE transformation rate at different initial PHE concentrations ($C_{aq,PHE}$). The slope of the regression line represents K_S/k_{max} and the y-intercept is $1/k_{max}$. The values for k_{max} and K_S are shown on the plot.

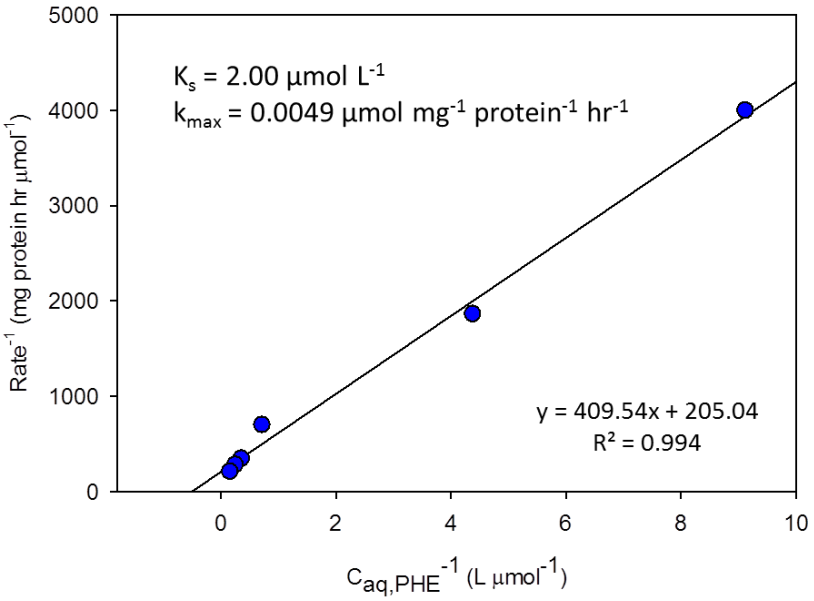

Methods

Maintaining *Mycobacterium* sp. strain ELW 1 Culture

Culture purity was ensured by plating liquid cultures on mineral salt medium (MSM) agar plates and storing the plates in an air-tight Oxoid™ Anaerobic 3.5 L Jar (ThermoFisher Scientific, #OXHP0011A) with ~1.5% isobutene (v/v), replenished weekly. MSM was prepared by combining 30 mL of Solution 1 (1 L ultra-high purity DIW with 20 g NH_4Cl, 0.7 g $MgCl_2 \cdot 6H_2O$, 1.0 g $(NH_4)_2SO_4$, and 2 mL of trace element solution (50 g Na EDTA, 22 g $ZnSO_4 \cdot 7H_2O$, 5.54 g $CaCl_2$, 5.06 g $MnCl_2 \cdot 4H_2O$, 4.99 g $FeSO_4$, 1.1 g $(NH_4)_6Mo_7O_{24} \cdot 4H_2O$, 1.57 g $CuSO_4 \cdot 5H_2O$, and 1.61 g $CoCl_2 \cdot 6H_2O$ in 1 L ultra-high purity DIW stored in refrigerator) autoclaved for 40 min) with 10 mL of Solution 2 (1 L ultra-high purity DIW with 155 g K_2HPO_4 and 85 g NaH_2PO_4 autoclaved for 40 min) into 270 mL autoclaved ultra-high purity DIW [3].

Protein Assay

ELW1 biomass was estimated by measuring the amount of cellular protein via a protein assay that has been previously published [4]. In brief, 15 mL of batch culture grown to >0.7 (OD_{600}) was centrifuged (15 mins at 9,000 rpm), reconstituted to 100 µL with deionized water, and transferred to 2 mL centrifuge tubes containing 100 µL of 3N NaOH. The cells were heated for 1hr at 75^{o}C then centrifuged (5 mins at 9,000 rpm). Plastic cuvettes were prepared with 100µL of sample supernatant, 100 µL 3N NaOH, 300 µL deionized water, and 500 µL MicroBiuret Reagent. The solution was allowed to react for 20 mins before measuring the absorbance at 540 nm. The amount of cellular protein in the batch culture was determined using a calibration curve and accounting for dilution during sample preparation.

Activity Tests

The activity of *Mycobacterium* sp. strain ELW1 was assessed by measuring the consumption of isobutene with time in batch reactors with liquid and gas components. The isobutene and oxygen must transfer from the gas phase to the liquid phase to be consumed by ELW1. To optimize its transfer between phases, 4.5 mL of MSM was used in 27 mL serum vials [5] and sealed with 20 mm Wheaton and 20 mm aluminum crimp caps. Calibration vials were prepared by spiking 150 µL, 200 µL, and 250 µL isobutene into the headspace of three separate vials. The batch reactor vials were spiked with 200 µL of isobutene into the headspace. Both the calibration and sample vials were allowed to equilibrate on a rotary shaker table at ~200 rpm at 30^{o}C. After equilibration, an aliquot of ~0.5 mL, or less, of cells re-suspended in MSM was added to the sample serum vials for a total cell mass of ~4 mg [6]. Immediate analysis of the isobutene concentration in the headspace was performed on a Hewlett Packard 6892 GC coupled to a FID with a GS-Q 30 m x 0.53 mm column (Agilent, Santa Clara, CA). The isothermal temperature program was held at 150^{o}C, with the inlet temperature set at 250^{o}C. Helium was used as the carrier gas with flow rate of 15 mL/min. The reactors were continuously shaken at 200 rpm to ensure mass transfer between the gas/liquid components. The total mass of isobutene consumed was determined by applying the Henry's Law. Isobutene has a dimensionless Henry's Law Constant of 10.06 at 30^{o}C.

Sensitivity of 1-Octyne Inactivation to Isobutene Oxidation

Terminal alkynes, particularly 1-octyne, has been shown to inactivate monooxygenase enzymes used in the oxidation of isobutene by ELW1 [3]. The sensitivity of various aqueous concentrations (C_{aq}) of 1-octyne, 2, 5, 10, and 11 µM, to ELW 1 was investigated. A bottle of gas-phase 1-octyne was prepared following [7]. Briefly, 40 µL of liquid 1-octyne (Sigma Aldrich, St. Louis, MO) was added to a 125 mL glass media bottle containing several glass beads and capped quickly with a black phenolic cap fitted with a new gray butyl septum. An additional 100 mL of ambient air was injected into the bottle to make a final stock concentration of 1 mM gas-phase 1-octyne. Necessary volumes of gas-phase 1-octyne stock were added to 27 mL serum vials containing 4.5 mL of MSM, 200 µL isobutene, and sealed with chlorobutyl septa and aluminum crimp caps. Vials were equilibrated on a rotary shaker table at ~200 rpm before adding ~0.5 mL (or less) of cells to the vials for a total cell mass of ~4 mg [6] and immediate analysis of isobutene concentration via GC/FID using the same system described in Activity Tests.

Analytical Method for the Measurement of Phenanthrene and Phenanthrene Metabolites

A. Extraction Method

All PHE transformation samples (5 - 15 mL) and toxicology samples (50 mL) from each of the 3 replicate bioreactors were extracted using solid phase extraction (SPE) with a modified version of a previously published method [8]. Bond Elut Plexa (30 mg, 3 mL) cartridges (Agilent Technologies, New Castle, DE) were preconditioned with 5

mL methanol, followed by 5 mL deionized water. The PHE transformation samples were spiked with phenanthrene-D_{10} and then added to cartridges and the eluent discarded. Metabolites retained on the cartridges were eluted with 5 mL acetone and 16 mL dichloromethane (DCM), dried with sodium sulfate, and concentrated using a TurboVap® evaporator (nitrogen gas, 30 °C water bath). The extracts from the PHE transformation samples were solvent exchanged to ethyl acetate and spiked with an internal standard to obtain a final volume of 300 µL. The toxicology samples were not spike with phenanthrene-D_{10} prior to SPE extraction following the same method described for the PHE transformation samples. Toxicology extracts were split gravimetrically 8:2 with 80% used for toxicology testing (referred to as toxicology fractions) and the remaining 20% used for chemical analysis (referred to as chemical fractions). Toxicology fractions were not blown to dryness and reconstituted with 100 µL dimethyl sulfoxide (DMSO) (Sigma Aldrich, St. Louis, MO) to a concentration of ~8 mmol PHE-equivalent L^{-1} DMSO. The chemical fractions were solvent exchanged to ethyl acetate and spiked with labeled surrogates and internal standards to obtain a final volume of 300 µL and analyzed for PHE and OHPAHs. The concentrations of PHE and OHPAHs measured in the chemical fractions were used to estimate concentrations in the toxicology fractions that were tested on zebrafish.

Estimated Detection Limits

Estimated Detection Limits (EDLs) for PHE and OHPHEs were calculated following EPA Method 8280 using equations (1) and (2):[9]

$$EDLs = \frac{(2.5)(C_{IS,S})(H_{n,S})}{(H_{IS,S})(RF)} \quad (1)$$

$$RF = \frac{(H_{x,std})(C_{IS,std})}{(C_{x,std})(H_{IS,std})} \quad (2)$$

Where $C_{IS,S}$ is the concentration of the internal standard in the sample, $H_{n,S}$ is the height of the noise in the sample, $H_{IS,S}$ is the peak height of the internal standard in the sample, RF is the response factor for the lowest calibration concentration for a particular analyte, $H_{x,std}$ is the peak height of the analyte in the lowest calibration standard, $C_{IS,std}$ is the concentration of the internal standard in the lowest calibration standard, $C_{x,std}$ is the concentration of the analyte in the lowest calibration standard, and $H_{IS,std}$ is the peak height of the internal standard in the lowest calibration standard.

Predication of Derivatized OHPAH Fragmentation Ions for GC/MS (EI)

Fragmentation ions were predicted according to a previously-described method [10] and listed in Appendix A.4. Briefly, the trimethylsilyl (TMS) group of BSTFA replaces the hydrogen in the hydroxyl group resulting in the addition of m/z 73 to the OHPAH, forming the molecular ion $[M]^+$ (Appendix A.6). Ionization by EI results in several cleavages including a methyl group $[M-15]^+$ and the TMS ether group ($OSi(CH_3)_3$) $[M-89]^+$. Additionally, cyclization of the TMS group with a carbon in the alpha position relative, to the silyl group, results in the loss of two methyl groups and one hydrogen $[M-31]^+$ (Appendix A.7). In a previous study, cyclization during derivatization was observed for 1-NAP, 1-PHE, 4-PHE, and 9-PHE [10] .

Toxicity of OHPHE metabolites

A. Cell Viability During PHE Exposure

Cell viability tests were performed on unexposed cells and PHE-exposed cells (including those exposed to 1-octyne) using Live/Dead cell staining and flow cytometry. Calibration standards (0.5 mL) with 0, 25, 50, 75, and 100% live cells were prepared by mixing different volume ratios of live and dead cells. Cells were grown in liquid media (described above) for 8 days (OD_{600} >0.7). Live cells (5 mL)

were mixed with an equal volume of 50 mM phosphate buffer. Dead cells were prepared by vortexing 5 mL of cells grown for 8 days with an equal volume of 90% ethanol. Fluorescent dye (SYTOX® Green Dead Cell Stain, # S34860, ThermoFisher Scientific, Waltham, MA) (0.5 µL) was added to each standard and allowed to incubate in the dark for 20 min during which only the dead cells, with compromised cell walls, are stained. Standards were analyzed with a BD Accuri™ C6 flow cytometer (BD Biosciences, San Jose, CA) using an analysis volume of 25 µL at a medium flow rate.

The distribution of live and dead cells was identified by differences in their fluorescence intensity; unstained live cells had low fluorescence intensity while the green-stained dead cells had high fluorescence intensity (Appendix B.4). The cut-off point between the live and dead cells fluorescence intensity was established by manually fitting a gating to the calibration standard on the cytometer software and applied to samples (Appendix B.4). A calibration curve was established from the ratio of live:dead cells and was used to determine the concentrations of live cells in experimental samples (Appendix B.5). Experimental samples were prepared and analyzed similarly to the standards except for the dilution step. Aliquots of 50, 100, or 250 µL were removed from the batch reactors and diluted to 0.5 mL with ultra-pure deionized water followed by the addition of 0.5 µL of fluorescent dye to achieve ~10,000 events μL^{-1}.

Bibliography

(1) Mackay, D.; Shiu, W. Y.; Ma, K.-C.; Lee, S. C., *Handbook of Physical-Chemical Properties and Environmental Fate for Organic Chemicals: Introduction and Hydrocarbons*. 2nd Edition ed.; Taylor & Francis Group: Boca Raton, FL, 2006; Vol. 1.

(2) Sander, R., Compilation of Henry's Law Constants (Version 4.0) for Water as Solvent. *Atmospheric Chemistry and Physics* **2015**, *15*, (8), 4399-4981.

(3) Kottegoda, S.; Wallgoram, E.; Hyman, M., Metabolism of 2-Methylpropene (Isobutylene) by the Aerobic Bacterium *Mycobacterium* Sp. Strain Elw1. *Journal of Applied and Environmental Microbiology* **2015**, *81*, (6), 1966-1976.

(4) Gornall, A. G.; Bardawill, C. J.; David, M. M., Determination of Serum Proteins by Means of the Biuret Reaction. *Journal of Biological Chemistry* **1949**, *177*, 751-766.

(5) Kim, Y.; Arp, D. J.; Semprini, L., A Combined Method for Determining Inhibition Type, Kinetic Parameters, and Inhibition Coefficients for Aerobic Cometabolism of 1,1,1-Trichloroethane by a Butane-Grown Mixed Culture. *Biotechnology and Bioengineering* **2002**, *77*, (5), 564-576.

(6) Rich, S. L. Kinetic Analysis of the Aerobic Degradation of Chlorinated Ethenes by the Mycobacterium Elw-1 and Chlorinated Ethanes and Ethenes by Rhodococcus Rhodochrous Atcc® 21198™. Oregon State University, Corvallis, Oregon, **2015**.

(7) Taylor, A. E.; Vajrala, N.; Giguere, A. T.; Gitelman, A. I.; Arp, D. J.; Myrold, D. D.; Sayavedra-Soto, L.; Bottomley, P. J., Use of Aliphatic *N*-Alkynes to Discriminate Soil Nitrification Activities of Ammonia-Oxidizing Thaumarchaea and Bacteria. *Journal of Applied and Environmental Microbiology* **2013**, *79*, (21), 6544-6551.

(8) Motorykin, O.; Schrlau, J.; Jia, Y.; Harper, B.; Harris, S.; Harding, A.; Stone, D.; Kile, M.; Sudakin, D.; Massey Simonich, S. L., Determination of Parent and Hydroxy Pahs in Personal Pm2.5 and Urine Samples Collected During Native American Fish Smoking Activities. *Science of The Total Environment* **2015**, *505*, 694-703.

(9) EPA Method - 8280a, Epa. The Analysis of of Polychlorinated Dibenzo-P-Dioxins and Polychlorinated Dibenzofurans by High-Resolution Gas Chromatography/Low Resolution Mass Spectrometry (Hrgc/Lrms).

(10) Schummer, C.; Delhomme, O.; Appenzeller, B. M. R.; Wennig, R.; Millet, M., Comparison of Mtbstfa and Bstfa in Derivatization Reactions of Polar Compounds Prior to Gc/Ms Analysis. *Talanta* **2009**, *77*, (4), 1473-1482.

Appendix B

Contents

Appendix B.1. Structure of phenanthrene depicting bay and K regions.

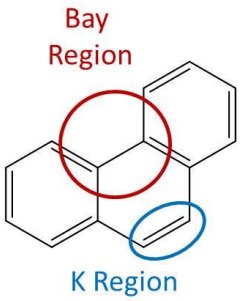

Appendix B.2. Example of derivatization reaction of BSTFA with 1-PHE.

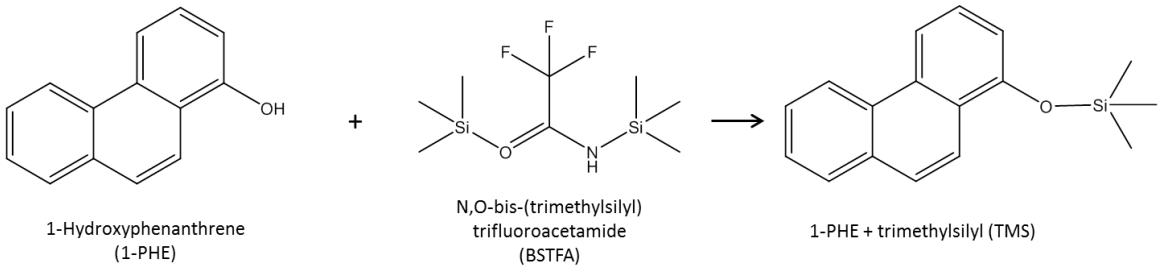

Appendix B.3. Example of cyclization of 1-PHE after derivatization with BSTFA.

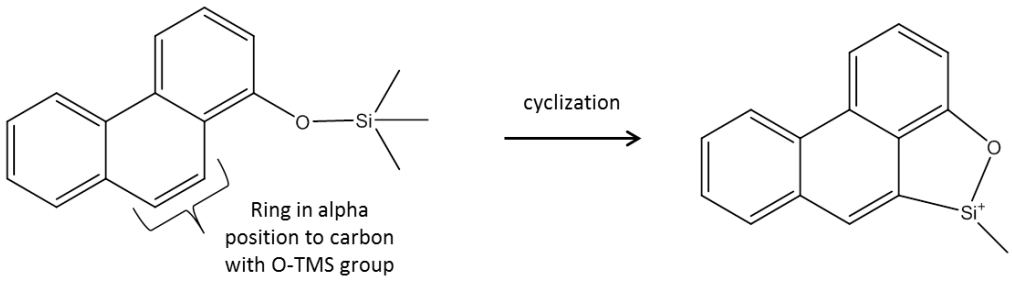

Appendix B.4. Distribution of live and dead ELW1 cells in calibration standards used to establish the gating for future samples. The plots on the right show the fluorescence intensity of the live cells (not stained) at ~630 nm (FL3-H) and of the dead cells stained green at ~510 nm (FL1-H). The plots on the right show the number of cells (Counts) versus the fluorescence intensity at ~510 nm with the unstained live cells showing a lower intensity of fluorescence compared to the green-strained dead cells. A: 100% live cells, 0% dead cells; B: 75% live cells, 25% dead cells; C: 50% live cells, 50% dead cells; D: 25% live cells, 75% dead cells; and E: 0% live cells, 100% dead cells.

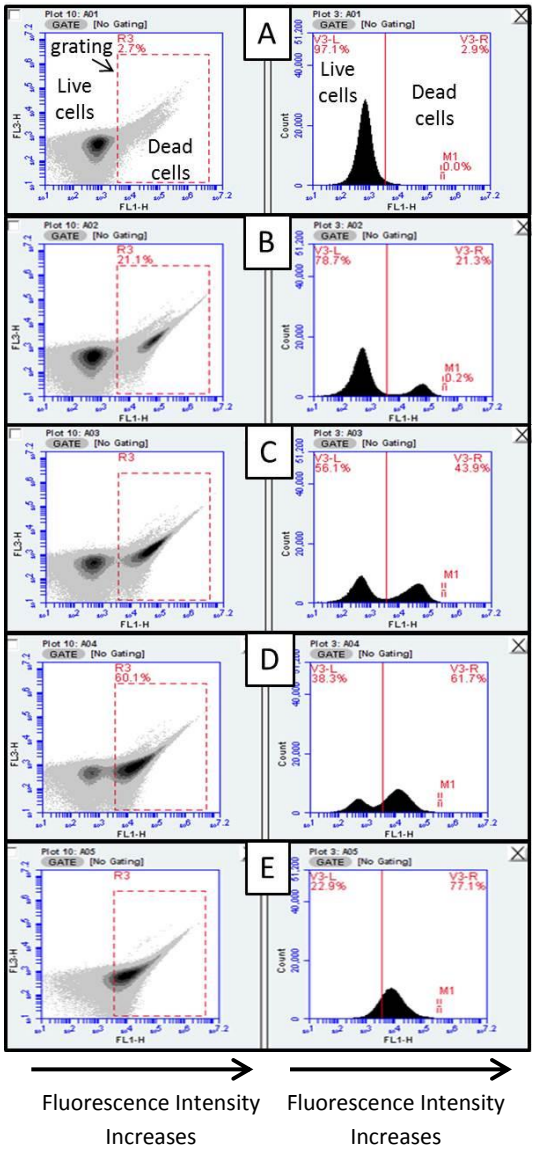

Appendix B.5. Calibration curve of Ratio of Live:Dead Cells versus % Live Cells.

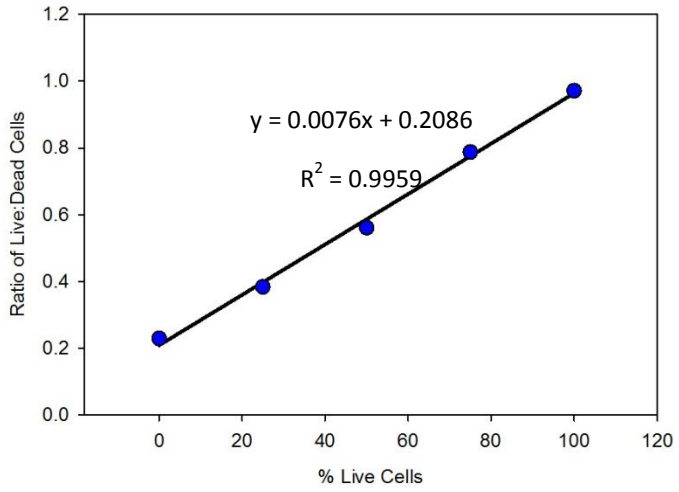

Appendix B.6 % Live cells (with standard error bars, *n* = 3 except for 0.84 µmol PHE, *n* = 2) from live/dead cell staining for 1-octyne controls, cell-only controls, and PHE-exposed cells at 0.42, 0.84, and 1.8 µmol PHE. Although there was some variability in % live cells in all the reactors, values were not statistically different over time or between the negative control, 1-octyne-inhibited positive control, or PHE- exposed cells.